

# Mammalian faunal change of the Miocene Dove Spring Formation, Mojave region, southern California, USA, in relation to tectonic history

### Fabian Cerón Hardy<sup>1,†</sup> and Catherine Badgley<sup>2,†</sup>

<sup>1</sup>University of Michigan, Department of Earth and Environmental Sciences, Room 2534, 1100 North University Avenue, Ann Arbor, Michigan 48109-1005, USA

### **ABSTRACT**

Tectonic processes drive the evolution of basins through local and regional changes in topographic relief, which have long-term effects on mammalian richness and distribution. Mammals respond to the resulting changes in landscape and climate through evolution, shifts in geographic range, and by altering their community composition. Here, we evaluate the relationship between tectonic episodes and the diversification history of fossil mammals in the Miocene Dove Spring Formation (12.5-8.5 Ma) of southern California, USA. This formation contains a rich fossil record of mammals and other vertebrates as well as structural and sedimentological evidence for tectonic episodes of basin extension, rotation, and translation.

We used several methods to compare the fossil record to the tectonic history of the Dove Spring Formation. We updated the formation's geochronology to incorporate current radiometric dating standards and measured additional stratigraphic sections to refine the temporal resolution of large mammal (>1 kg) fossil localities to 200-kyr (or shorter) intervals. Observed species richness over time follows the same trend as the number of localities and specimens, suggesting that richness reflects sampling intensity. Estimates of stratigraphic ranges with 80% confidence intervals were used to conduct per capita diversification analysis and a likelihood approach to changes in faunal composition from one time interval to the next. While edge effects influence time bins at the beginning and end of the study interval, we

Fabian Cerón Hardy https://orcid.org/0000 -0002-9000-7227

Catherine Badgley https://orcid.org/0000-0002

 $^\dagger hardyf@umich.edu; cbadgley@umich.edu$ 

found changes in diversification rates and faunal composition that are not solely linked to preservation. Several rare species appear at 10.5 Ma and persist through the top of the formation despite variable preservation rates. Changes in faunal composition at 12.1 Ma and 10.5 Ma are not associated with elevated preservation rates, which indicates that some faunal changes are not primarily driven by sampling effort. The lower portion of the formation is characterized by high origination rates and long residence times. The upper portion has high per capita extinction rates that increased in magnitude as basin rotation and translation progressed from 10.5 Ma. The greatest change in faunal composition coincided with basin rotation and translation that interrupted a long-running extensional period. Tectonics played key roles in the diversity of mammals by determining fossil productivity and shaping the landscapes that they inhabited.

### INTRODUCTION

Local and regional tectonic processes have a direct influence on climatic gradients and vegetation patterns relevant to animals, influencing their evolution, distribution, and community composition (Janis, 1993; Kohn and Fremd, 2008; Eronen et al., 2015). The fossil record can reveal the response of mammalian communities to these environmental influences, as seen in sedimentary basins throughout the Basin and Range Province of western North America (Badgley and Finarelli, 2013; Smiley et al., 2018; Loughney et al., 2021). Tectonic processes throughout the middle Miocene included widespread extension and major topographic changes that led to the development of topographically complex landscapes that characterize the region today (Dickinson, 2002; McQuarrie and Wernicke, 2005; Bahadori et al., 2018). High mammalian

species richness at the regional scale is associated with this period of tectonic development, and a similar pattern may be detectable at the basin scale (Loughney et al., 2021). Here, we focus on the middle to late Miocene Dove Spring Formation (12.5–8.5 Ma), which is located in the El Paso Basin of the northwestern Mojave region in southern California, USA (Fig. 1).

The deposition of the Dove Spring Formation coincided with a period of global changes in climate that began around 14 Ma known as the Middle Miocene Climatic Transition (MMCT; Zachos et al., 2001; Frigola et al., 2018; Steinthorsdottir et al., 2021). Regional tectonic episodes altered elevation and topographic relief in western North America, leading to increased seasonality of temperature and precipitation compared to the warmer Middle Miocene Climatic Optimum (ca. 17-14 Ma). Faunal assemblages characterized, in part, by high species richness of ungulates developed throughout the Basin and Range in response to tectonically driven climatic and vegetation gradients of the MMCT (Wing, 1998; Janis et al., 2000; Chamberlain et al., 2014).

We investigated the links between tectonic history and mammalian species richness through geologic time with three goals: (1) to refine the stratigraphy and geochronology to serve as a temporal framework for evaluating faunal change in relation to tectonic episodes, (2) to identify changes in species richness and composition based on the estimated residence time of large mammals, and (3) to assess per capita origination and extinction rates in relation to the timing of tectonic episodes. Our work is part of a broader effort to examine changes in landscape, climate, vegetation, and mammalian diversity that are associated with tectonic processes occurring throughout western North America (Finarelli and Badgley, 2010; Badgley and Finarelli, 2013; Badgley et al., 2017; Loughney and Badgley, 2020). Previous work in the Crowder, Cajon Valley, and Barstow formations

GSA Bulletin; published online 6 November 2023 https://doi.org/10.1130/B37082.1.

<sup>&</sup>lt;sup>2</sup>University of Michigan, Department of Ecology and Evolutionary Biology, 1105 North University Avenue, Biological Sciences Building, Ann Arbor, Michigan 48109-1085, USA

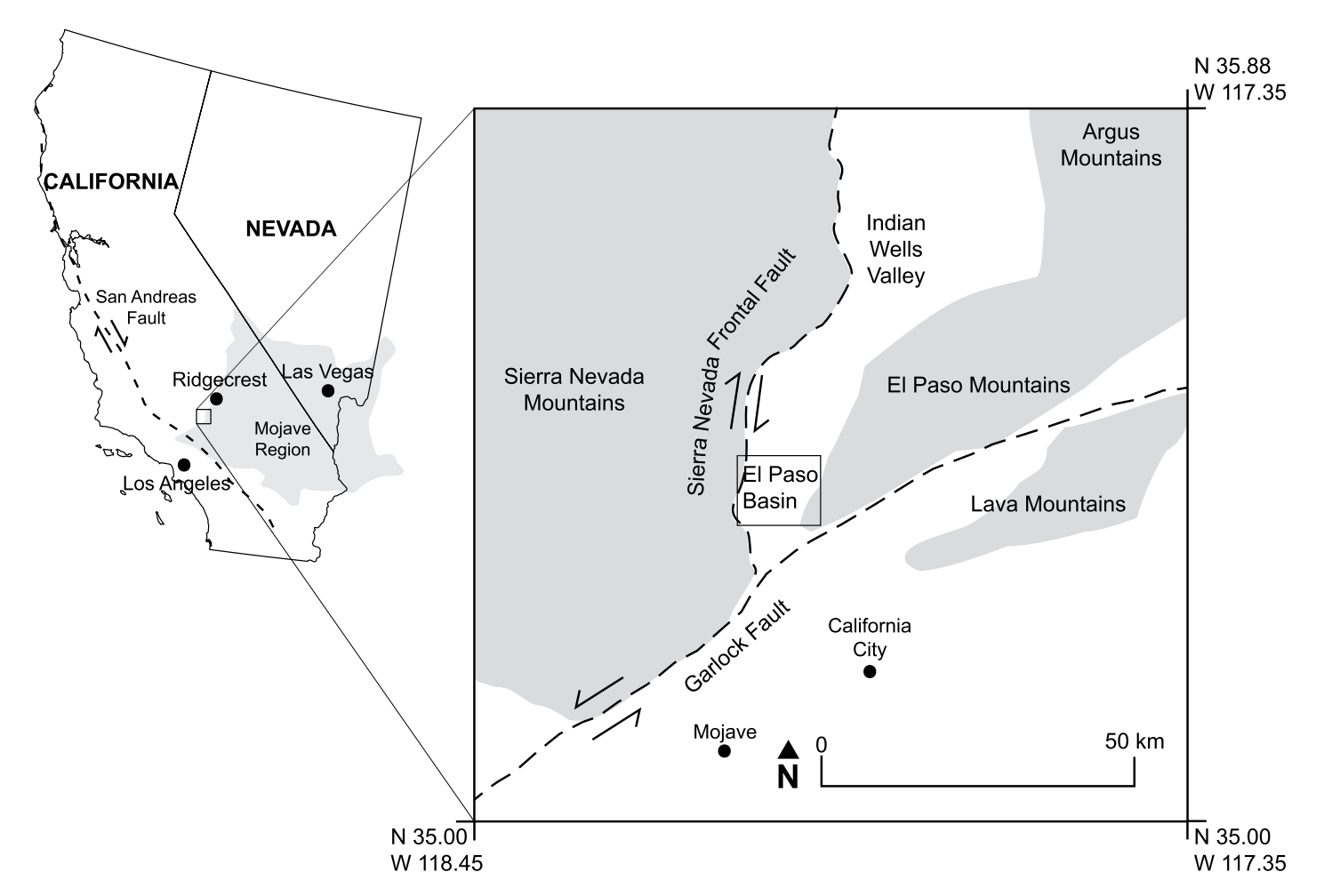


Figure 1. Map of study location, centered on the El Paso Basin. The basin's southern boundary is the Garlock fault, and the western boundary is the frontal fault of the Sierra Nevada Range.

within the Mojave region has illustrated patterns of increased species richness in topographically complex landscapes that are not driven by preservation (Smiley, 2016; Loughney and Badgley, 2020; Loughney et al., 2021).

### Paleontological Background

The Dove Spring Formation is located in the El Paso Basin of southern California, USA (35.373° N, 117.991° W). This formation spans Clarendonian (12.5–10.3 Ma) to early Hemphillian (10.3–8.5 Ma) North American land mammal ages. These intervals of geologic time are characterized, in part, by decreasing species richness of ungulate taxa (Woodburne, 1987, 2004; Janis et al., 2000). The Dove Spring Formation has been well studied in terms of vertebrate paleontology, lithostratigraphy, tephrochronology, and tectonic setting (Merriam, 1919; Dibblee, 1967; Loomis and Burbank, 1988; Whistler and Burbank, 1992; Perkins et al., 1998; Wang and Barnes, 2008). Over 7400 vertebrate fossils have

been collected and catalogued from more than 750 localities by workers associated with the Natural History Museum of Los Angeles County for over a century, leading to a well-documented sequence of mammalian assemblages (Tedford et al., 2004; Whistler et al., 2009). Over 100 mammalian species have been recognized in the Dove Spring Formation, 70 of which are largemammal lineages (>1 kg in estimated adult body weight; Whistler et al., 2009). Four orders (Artiodactyla, Carnivora, Perissodactyla, and Proboscidea) and 14 families of large mammals are recognized in the Dove Spring Formation, with 59 taxa identified to the genus level and 20 further identified to the species level. (Here, we refer to the taxonomic order "Artiodactyla" due to its priority over "Cetartiodactyla" as a monophyletic group that includes the last common ancestors of all even-toed ungulates in this study; Asher and Helgen, 2010; Prothero et al., 2022.)

Ungulates are well represented in the Dove Spring Formation. Artiodactyl families include Antilocapridae (pronghorns), Camelidae (camels), Merycoidodontidae (oreodonts), and Tayassuidae (peccaries) (Whistler and Burbank, 1992; Whistler et al., 2009). Antilocaprids are represented by four genera and are the most commonly occurring artiodactyls in terms of specimens and localities. Camelids are represented by three genera and numerous specimens. Merychyus major is the only species of merycoidodontid present. Tayassuids are rare in the formation and are represented by *Prosthennops* sp. Perissodactyls in the formation belong to the Equidae (horses) and Rhinocerotidae (rhinos), with equids represented by numerous specimens from seven species, while rhinocerotids are rare and limited to one genus (Apehlops). Proboscideans belong to two families, Amebelodontidae and Gomphotheriidae, and are represented by one species each (Amebelodon burnhami and Gomphotherium sp., respectively). Canids are the most common carnivores, with nine lineages recognized in the formation, six of which belong to the Borophaginae (bone-crushing dogs; Wang and Barnes, 2008; Tedford and Wang, 2009). The Amphicyonidae are represented by *Ischyrocyon mohavensis*, which occurs alongside canids through most of the formation. Three species of Felidae are present, but their fossils are considerably rarer than those of the Canidae (Whistler et al., 2009; Tseng et al., 2010). The Barbourofelidae are rare and represented by *Barbourofelis whitfordi*. Four mustelid species are present (Whistler and Burbank, 1992; Whistler et al., 2009). Tedford (1965) divided the fossil record of the Dove Spring Formation into three superposed faunal assemblages that were later revised with new age interpretations by Whistler et al. (2009).

We used the fossil record of large mammals to evaluate potential causes of faunal change, particularly tectonic changes in the basin and regional climate. Changes in per capita rates of origination and extinction can be detected by analyzing taxonomic richness through a stratigraphic sequence. Using statistical estimates of residence times of lineages, we generated a record of estimated richness and faunal composition that provides a more realistic chronology of faunal history compared to the observed fossil record. We focus on the large mammals of the Dove Spring Formation because they are the most abundant group among the fossil assemblages in terms of specimens recovered and species richness (Table 1).

### Geologic Background

The Dove Spring Formation is the upper member of the Ricardo Group and consists of 1800 m

of fluvial and lacustrine sediments and volcanic ashes deposited between 12.5 Ma and 8.5 Ma (Fig. 2; Whistler and Burbank, 1992; Whistler et al., 2009). It lies disconformably above the predominantly volcanic Cudahy Camp Formation (ca. 18–15 Ma: Loomis and Burbank, 1988: Whistler et al., 2009). The study interval mostly consists of sandstones and mudstones interbedded with at least 18 laterally extensive ash units (Loomis and Burbank, 1988; Whistler and Burbank, 1992; Perkins et al., 1998). Dating methods include magnetostratigraphy, tephrochronologic correlation, and radiometric dating (U-Pb, K/Ar, <sup>40</sup>Ar/<sup>39</sup>Ar, and fission-track dating) and provide a temporal resolution of  $\sim$ 200,000 years to most fossil localities (Evernden et al., 1964; Tedford, 1965; Cox and Diggles, 1986; Loomis and Bur-

TABLE 1. LARGE MAMMALS OF THE DOVE SPRING FORMATION WITH OBSERVED AND ESTIMATED FIRST AND LAST OCCURRENCES

Group	Species	Obs. first occ. (Ma)	Obs. last occ. (Ma)	Est. first occ. (Ma)	Est. last occ. (Ma)	No. of fossil horizons
<del></del>	Species	ODS. HIST OCC. (Ma)	ODS. IdSt OCC. (IVIA)	ESt. IIISt OCC. (IVIA)	ESI. IASI OCC. (IVIA)	140. 01 105511 1101120115
Artiodactyla	Unassigned*	12.5	8.5	12.7	8.3	21
Antilocapridae		12.5 8.7	8.7		8.7	1
Antilocapridae	cf. Illingoceros sp.			8.7		
Antilocapridae	Cosoroyx sp.	12.3	8.9	12.6	8.6	14
Antilocapridae	Paracosoryx furlongi	12.5	10.9	12.7	10.7	8 8
Antilocapridae	Plioceros sp.	10.5	8.9	10.7	8.7	
Camelidae	Unassigned*	12.5	8.5	12.7	8.3	21
Camelidae	Aepycamelus sp.	10.5	9.5	10.8	9.2	4
Camelidae	Megatylopus sp.	10.3	9.5	10.5	9.3	5 5 7
Camelidae	Procamelus sp.	11.1	9.9	11.4	9.6	5
Merycoidodontidae	Unassigned	12.3	8.7	12.9	8.1	
Merycoidodontidae	Merychyus major	12.5	8.9	12.9	8.5	11
Tayassuidae	Unassigned	10.9	9.9	11.2	9.7	5
Tayassuidae	Prosthennops sp.	11.1	10.1	11.6	9.6	3
<u>Perissodactyla</u>						
Equidae	Unassigned*	12.5	8.5	12.7	8.3	21
Equidae	Cormohipparion sp.	11.9	9.5	12.1	9.3	12
Equidae	"Dinohippus" leardi	11.1	8.7	11.5	8.3	7
Equidae	Hipparion forcei	11.7	8.7	12.0	8.4	11
Equidae	<i>Hipparion</i> sp.	12.3	8.7	12.6	8.4	12 7
Equidae	Hipparion tehonense	11.1	9.7	11.3	9.5	
Equidae	Megahippus sp.	12.5	10.5	13.5	9.5	3
Equidae	Pliohippus tantalus	12.5	8.5	12.8	8.3	17
Rhinocerotidae	Unassigned	11.9	8.7	12.3	8.3	9
Rhinocerotidae	Aphelops sp.	11.9	9.9	12.6	9.2	4
Proboscidea						
Proboscidea Proboscidea	Unassigned	11.1	8.9	11.7	8.4	5
Amebelodontidae	Amebelodon burnhami	11.1	8.9	11.7	8.4	5 5
Gomphotheriidae	Unassigned	12.5	8.7	12.8	8.4	16
Gomphotheriidae	Gomphotherium sp.	12.3	8.7	12.6	8.4	13
·	от при том том том том					
Carnivora	Unaccionad	10.0	0.0	10.6	0.6	10
Carnivora	Unassigned	12.3	8.9 9.3	12.6	8.6	12
Amphicyonidae	Ischyrocyon mohavensis	12.1		13.5	7.9	3 3
Barbourofelidae	Barbourofelis sp.	10.5	9.5	11.0	9.0	
Barbourofelidae	Barbourofelis whitfordi	9.7	9.7	9.7	9.7	1
Canidae	Unassigned	12.1	8.7	12.4	8.4	14
Canidae	Borophagus littoralis	10.5	8.9	11.0	8.4	4
Canidae	Carpocyon robustus	11.1	9.7	12.5	8.3	2 1
Canidae	Carpocyon webbi	8.9	8.9	8.9	8.9	
Canidae	Epicyon haydeni	10.5	9.7	10.9	9.3	3
Canidae	Epicyon saevus	12.1	8.9	12.7	8.3	6
Canidae	Epicyon sp.	10.3	9.7	10.5	9.5	4
Canidae	Leptocyon vafer	11.3	8.9	12.1	8.1	4 4
Canidae	Metalopex macconnelli	9.7	8.7	10.0	8.4	
Canidae	Vulpinae	8.7	8.7	8.7	8.7	1
Felidae	Unassigned	12.5	8.9	13.0	8.5	9
Felidae	Homotherium sp.	10.3	8.9	11.0	8.2	3
Felidae	<i>Nimravides</i> sp.	10.3	10.3	10.3	10.3	1
Felidae	Pseudaelurus sp.	9.9	9.5	10.3	9.1	2
Mustelidae	Unassigned	10.5	8.7	10.9	8.3	6 5
Mustelidae	Martes buwaldi	10.5	8.7	11.0	8.3	5
Mustelidae	Martinogale faulli	9.9	8.7	10.5	8.1	3
Procyonidae	Bassariscus sp.	10.1	8.7	10.5	8.4	5

Note: In cases where species-level identification was not available for a time interval, we counted fossils identified to the family-level as species lineages to indicate the presence of a group. Fossil horizons represent the number of 200-kyr time bins from which any particular taxon has been recovered. Obs.—Observed; occ.—occurrence; Est.—Estimated; No.—Number.

<sup>\*</sup>These taxa were excluded from most of our diversification analyses because they span nearly the entire formation and do not contribute meaningful information.

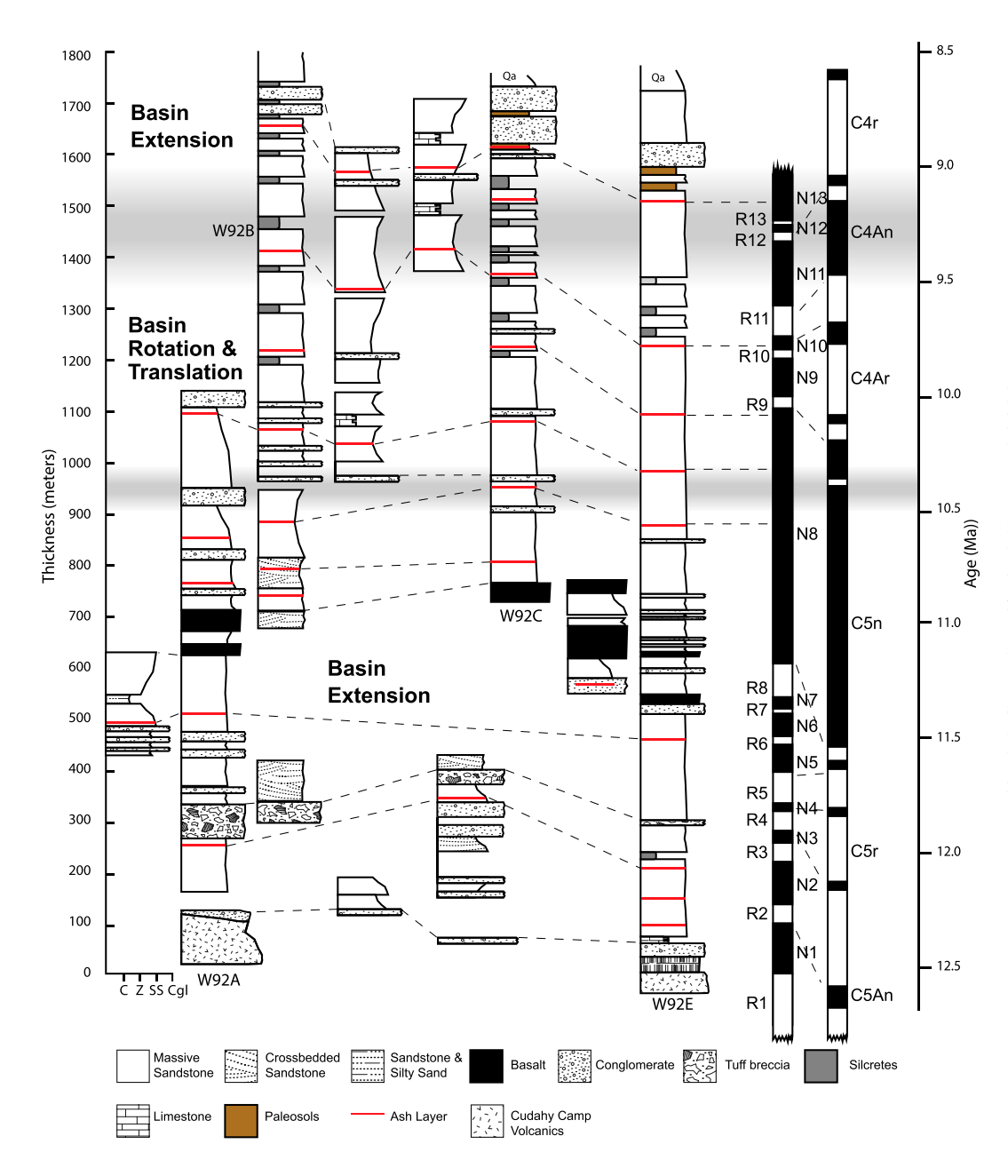


Figure 2. Stratigraphy of the Dove Spring Formation with updated correlations based on recalibrated radiometric dates. Top of formation is based on new tephrochronologic correlation by Knott et al. (2022). Columns labeled W92 are modified from Whistler and Burbank (1992). Magnetic polarity stratigraphy is from Whistler et al. (2009). Magnetic polarity time scale is modified from Hilgen et al. (2012). Lateral distance between first and last columns is  $\sim$ 8 km.

bank, 1988; Whistler and Burbank, 1992; Perkins et al., 1998; Perkins and Nash, 2002; Smith et al., 2002; Lourens et al., 2004; Tedford et al., 2004; Bonnichsen et al., 2008; Whistler et al., 2009; Table 2). The lower half of the formation contains two thick basalt flows, with a  $^{40}\mathrm{Ar}/^{39}\mathrm{Ar}$  radiometric age of 10.5  $\pm$  0.25 Ma measured in the upper basalt (Loomis and Burbank, 1988; Whistler and Burbank, 1992).

Analysis of faunal and environmental changes requires a well-resolved chronology. The current chronological framework for the Dove Spring Formation is the culmination of decades of work integrating lithostratigraphy, magnetostratigraphy, biostratigraphy, and tephrochronology of the formation. Ten of the 18 prominent ashes in

the study area were correlated throughout western North America using tephrochronology, and the remaining eight were radiometrically dated (Perkins et al., 1998; Perkins and Nash, 2002). Improvements to radiometric methods necessitate occasional revisions to age estimates to ensure accuracy and consistency (Begemann et al., 2001; Renne et al., 2010; Carter et al., 2020; Schaen et al., 2021). Ages of many fossil localities are based on the tephrochronology of associated ash layers (Whistler et al., 2009, 2013). To further refine the stratigraphic resolution and age estimates of fossil localities, we measured 19 new stratigraphic sections and updated magnetostratigraphic correlations to the 2012 edition of the Geomagnetic Time Scale (Whistler and Burbank, 1992; Hilgen et al., 2012). We updated 18 published radiometric dates for the Dove Spring Formation using current decay-constant standards (Begemann et al., 2001; Renne et al., 2010; Carter et al., 2020).

The El Paso Basin is located within a large fault zone that separates the western Basin and Range from the Sierra Nevada Mountains. The Walker Lane Belt and the Eastern California Shear Zone are right-lateral, strike-slip fault zones separated by the left-lateral Garlock fault (Loomis and Burbank, 1988; Faulds and Henry, 2008; Andrew et al., 2015; Dixon and Xie, 2018). These fault zones accommodate boundary motion between the Pacific and North American tectonic plates (Guest et al., 2007).

TABLE 2. RADIOMETRIC DATES OF PROMINENT AND LATERALLY CONTINUOUS ASH LAYERS WITHIN THE DOVE SPRING FORMATION, WITH UPDATED DECAY CONSTANTS

Ash number	Date (Ma)	Error (± m.y.)	Radiometric system	Tephra correlation	Date using updated decay constant (Ma)	Difference (m.y.)	Source
17	8.7945	0.1945	_	Monterey Fm.	_	_	Knott et al. (2022)
16	8.5	0.15	40Ar/39Ar		8.52	+0.02	Whistler and Burbank (1992)
15	8.4	1.8	FT	_	8.42	+0.02	Cox and Diggles (1986)
14	N.D.	_	_	_	_	· —	N.A.
13	N.D.	_	_	_	_	_	N.A.
12	N.D.	_		— O-1-t 0		<del>-</del>	N.A.
11	9.7	0.2	40Ar/03Ar	Celetron 2	9.72	+0.02	Perkins et al. (1998); Perkins and Nash (2002); Bonnichsen et al. (2007)
10	N.D.	_	<del>-</del> .	_	_	_	N.A.
9	10.2	0.2	<sup>40</sup> Ar/ <sup>39</sup> Ar	OC3	10.22	+0.02	Perkins et al. (1998); Perkins and Nash (2002); Bonnichsen et al. (2007)
8	10.6	0.2	<sup>40</sup> Ar/ <sup>39</sup> Ar	OC2	10.62	+0.02	Perkins et al. (1998); Perkins and Nash (2002); Bonnichsen et al. (2007)
7	10.4	1.6	FT	_	10.42	+0.02	Cox and Diggles (1986)
N.A.	10.5	0.25	40Ar/39Ar	Basalt	10.52	+0.02	Whistler and Burbank (1992)
7	11.01	0.03	<sup>40</sup> Ar/ <sup>39</sup> Ar	CPT XIII	11.03	+0.02	Perkins et al. (1998); Perkins and Nash (2002); Bonnichsen et al. (2007)
6	10.5	0.25	40Ar/39Ar	_	10.52	+0.03	Whistler and Burbank (1992)
5	11.2	0.1	<sup>40</sup> Ar/ <sup>39</sup> Ar	CPT XII	11.23	+0.03	Perkins et al. (1998); Perkins and Nash (2002); Bonnichsen et al. (2007)
4	11.64	0.05	_	Ammonia Tanks	11.67	+0.03	Perkins et al. (1998); Bonnichsen et al. (2007)
3	11.8	0.9	FT	_	11.83	+0.03	Loomis and Burbank (1988)
3	11.83	0.05	_	Rainier Mesa	11.86	+0.02	Perkins et al. (1998); Bonnichsen et al. (2007)
2	11.7	0.2	<sup>40</sup> Ar/ <sup>39</sup> Ar	_	11.55	<sup>+0.02</sup> −0.15	Smith et al. (2002)
2	12.01	0.03	<sup>40</sup> Ar/ <sup>39</sup> Ar	Ibex Hollow	12.04	+0.03	Perkins et al. (1998); Perkins and Nash (2002); Bonnichsen et al. (2007)
1	10.3	_	K/Ar	_	10.32	+0.02	Evernden et al. (1964)
1	12.15	0.04	<sup>40</sup> Ar/ <sup>39</sup> Ar	CPT V	12.18	+0.02 +0.03	Perkins et al. (1998); Bonnichsen et al. (2007)
0	15.1	0.5	K/Ar	_	15.13	+0.03	Cox and Diggles (1986)

Note: Radiometric dates of prominent and laterally continuous ash layers within the Dove Spring Formation. All dates were updated with currently accepted radioactive decay constants. N.A.—not applicable; N.D.—no data; Fm.—formation; FT—fission-track dating.

The fault geometry within the El Paso Basin displays characteristics of both extensional and shear movement. Loomis and Burbank (1988) recognized four episodes of structural development in the basin. During episode 1, the underlying Paleocene Goler Formation was tilted between the late Paleocene and early Miocene. Episode 2 is a period of north-south extension that began during the deposition of the underlying Cudahy Camp Formation (approximately 18-15 Ma). A series of east-west trending dikes within the Cudahy Camp Formation is associated with northwest movement between 17 Ma and 15 Ma of an extensive area of bedrock known as the Sierra Nevada-Great Valley crustal block (McQuarrie and Wernicke, 2005; Camp et al., 2015). This long episode of extension continued to increase the basin area and created accommodation space for sediment accumulation during the first 2.5 m.y. of the Dove Spring Formation. Episode 3 began at ca. 10.5 Ma with counterclockwise rotation of the basin and allowed for westward translation of the entire basin along the Garlock fault up to 64 km closer to the Sierra Nevada. In episode 4, west-northwest tilting and related extension deformed strata as young as 9.0 Ma, increasing subsidence and basin relief relative to the Sierra Nevada Mountains.

As the extension taking place during episode 2 progressed during the early deposition of the Dove Spring Formation, the basin increased in

size relative to episode 1. Increasing subsidence allowed for the development of mature southeastto-northwest drainage networks that transported sediments from the El Paso Mountains into the basin (Loomis and Burbank, 1988). Lacustrine sediments are present in the northern part of the basin underneath the basalts, and lakes are common features in extensional settings (Gawthorpe and Leeder, 2000). The isotopic signal of a rain shadow east of the Sierra Nevada Mountains documented since 16.0 Ma in several locations throughout the Great Basin indicates that there was significant relief between the southern Sierra Nevada and the northwestern Mojave region during the early deposition of the Dove Spring Formation (Loomis and Burbank, 1988; Poage and Chamberlain, 2002; Crowley et al., 2008; Whistler et al., 2009). This rain shadow began to weaken during episode 2 as regional extension lowered the paleoelevation of the southern Sierra Nevada (Poage and Chamberlain, 2002; Lechler et al., 2013). In addition, pollen and diatom records from the contemporaneous marine Monterey Formation indicate that the regional climate during tectonic episode 2 began turning cooler and drier at 15 Ma (Flower and Kennett, 1993; Heusser et al., 2022).

The rotation and translation of episode 3 coincided with increasing subsidence rates throughout the central Basin and Range (Andrew et al., 2015; Loughney et al., 2021). Movement along

the Garlock fault during this interval is partially constrained by volcanism in the Summit Range east of the El Paso Basin, with lithological and geochemical correlations that suggest close proximity to the Lava Mountains until ca. 10.3 Ma (Fig. 1; Smith et al., 2002; Andrew et al., 2015). The initiation of movement on this segment of the Garlock fault accommodates slip between the Walker Lane Belt to the north and the Eastern California Shear Zone to the south. Fault movement is correlated with changes in sediment accumulation rate, and an age of 10.5 Ma allows for uncertainty in estimating the timing of its initiation (Mitchell and Reading, 1978; Loomis and Burbank, 1988; Burbank and Anderson, 2012). The tectonic activities of episode 3 locally interrupted the steady rates of subsidence within the basin and may have cut off existing drainage channels (Loomis and Burbank, 1988; Gawthorpe and Leeder, 2000). The regional cooling and drying trends observed within the Monterey Formation that began during episode 2 continued into tectonic episode 3 (Flower and Kennett, 1993; Heusser et al., 2022).

Episode 4 represents a new period of eastwest extension in the El Paso Basin that began between 9.5 Ma and 9.0 Ma based on cut strata and progressively less rotation observed in beds younger than 10.0 Ma (Loomis and Burbank, 1988). Concurrent regional extension was associated with the southward migration of the

Rivera triple junction as the San Andreas transform boundary between the Pacific and North American plates shifted toward the current Gulf of California (Dickinson, 2002; McQuarrie and Wernicke, 2005; Bahadori et al., 2018). Dove Spring sediments from episode 4 are increasingly coarse, with distinctively granitic clast composition that indicates the Sierra Nevada Mountains to the west were a new sediment source by 9.0 Ma (Loomis and Burbank, 1988; Fig. 2). Paleocurrent studies by Loomis and Burbank (1988) demonstrated a shift to a northwestto-southeast drainage pattern, and the coarser sediments suggest the presence of higher-energy stream channels than during the extension of episode 2. Mean annual precipitation began to increase after 8.9 Ma throughout the region based on macrofossil and pollen records from several nearby basins that indicate the expansion of water-reliant pine forests (Axelrod, 1977; Heusser et al., 2022). Regional extension during episode 4 may have further weakened the rainshadow effect from the southern Sierra Nevada, although there is debate regarding the precise timing of changes to its paleoelevation (Poage and Chamberlain, 2002; Lechler et al., 2013).

### DATA AND METHODS

To investigate the potential link between tectonic episodes and fossil preservation, we used a composite stratigraphic column to calculate average sediment accumulation rates throughout the Dove Spring Formation. Variations in sediment accumulation rate are indicators of changes in topography or subsidence that influence the preservation potential of sediments (Rust and Koster, 1984; Paola et al., 1992; Finarelli and Badgley, 2010; Loughney et al., 2021). In terrestrial basins, this rate is controlled by changes in subsidence driven largely by fault movement resulting in subsidence or changes in relief (Leeder, 1993; Holland, 2016; Holland and Loughney, 2021). We utilized data for the stratigraphic thickness of each magnetic polarity interval and the thickness between dated ash deposits to calculate sediment accumulation rates. We omitted the pair of thick basalt flows near the middle of the section from our calculations because these volcanic units are not part of the normal mode of deposition.

We assigned fossil localities to 200-kyr time bins and developed a biochronology based on fossil occurrences within these intervals. We followed the convention of naming time bins based on the beginning of each bin (e.g., 12.50–12.31 Ma; 12.3–12.11 Ma). We placed fossil localities into accurate geographic and stratigraphic contexts by reviewing a series of 24 aerial photographs, 15 field notebooks, seven

topographic maps, and three geologic maps produced by David Whistler of the Natural History Museum of Los Angeles County (Los Angeles, California, USA) during his extensive work on the Dove Spring Formation. GPS technology did not exist at the time of collection for many of these localities, so Whistler and colleagues used topographic and geologic maps in conjunction with U.S. Geological Survey aerial photographs to document localities on the ground. We georeferenced these maps and photographs using the North American Datum of 1983 (NAD 83) as a spatial reference to place localities in Google Earth and Esri's ArcGIS. We measured 19 new stratigraphic sections in the field and used stratigraphic marker units to correlate them to the stratigraphy of Whistler and Burbank (1992), Whistler et al. (2009), and Whistler et al. (2013) to refine the stratigraphic placement of fossil localities throughout the formation.

The Natural History Museum of Los Angeles County vertebrate paleontology database contains over 7200 specimens recovered from the Dove Spring Formation. The majority (6747) of these specimens are fossil mammals, with the remainder consisting of reptiles, amphibians, birds, and fish. We compiled a faunal list of large mammal specimens identified to the species, genus, or family level for a total of 49 taxa that span the 4 m.y. of stratigraphic record. In some cases, specimens are identified to the genus or family level but cannot be assigned to a single species. These specimens still provide valuable occurrence data, so we established criteria for their inclusion in our analyses. When a genus is represented by multiple species, unassigned specimens could belong to any of those species, so we omitted these from further analysis. In cases in which a genus is represented by a single species, unassigned specimens were only counted as separate species lineages when species-level identification was not possible. Family-level designations were only included as species lineages when their estimated residence times did not span the entire formation.

The true residence time of any fossil taxon is underrepresented by observed specimens due to incomplete preservation. To account for the uncertainty in observed stratigraphic ranges, we used the method of Strauss and Sadler (1989) to calculate 80% confidence intervals based on the number of time intervals containing each taxon. We selected this confidence level to maintain resolution on the timing of originations and extinctions through the formation while acknowledging the sampling density of large mammal specimens (n = 3648). This method assumes a constant probability of recovering a fossil from within a taxon's true stratigraphic range. We calculated the unbiased point estimates of first and

last occurrences of each large mammal lineage by adding the average gap size between fossil horizons to the observed first and last occurrences in 200-kyr time bins (Table 1). Most of our analyses are based on the estimated residence times (Fig. 3). Confidence intervals and point estimates were not calculated for singletons, as these estimates require multiple horizons.

An important consideration in our analyses is the presence of edge effects (Foote, 2000; Badgley and Finarelli, 2013). This phenomenon is due to the limitations of the fossil record to capture taxa whose residence times actually extend beyond the study interval and is strongly influenced by the presence of singletons, which we excluded from our analyses. Observed richness is typically low near both the beginning and end of any study interval, with high numbers of first appearances toward the lower edge and last appearances toward the upper edge (Alroy, 2010). Edge effects result in inflated per capita rates of origination at the start of an interval and inflated per capita rates of extinction at the end. To mitigate the influence of edge effects, we excluded the first two and last two time intervals (12.5 Ma, 12.3 Ma, 8.7 Ma, and 8.5 Ma) from our interpretations of faunal change. This allowed us to acknowledge the presence of edge effects while focusing on internal richness patterns.

Following Strauss and Sadler (1989; also Marshall, 1990, 2010), the formula for calculating a stratigraphic range extension using an 80% confidence interval is:

$$r_c = R[(1-C)^{-1/(H-1)} - 1],$$
 (1)

where:

 $r_c$  = projected stratigraphic range extension,

R = observed stratigraphic range (observed first occurrence datum - observed last occurrence datum).

C = confidence level (80% in this study), and

H = number of time intervals with occurrence of taxon

The average gap size between fossil occurrences is given in the following equation:

$$r_{unbiased} = R/(H-1),$$
 (2)

where:

 $r_{unbiased}$  = average gap size between fossil

R = observed stratigraphic range (observed first occurrence datum – observed last occurrence datum), and

H = number of time intervals with occurrence of taxon.

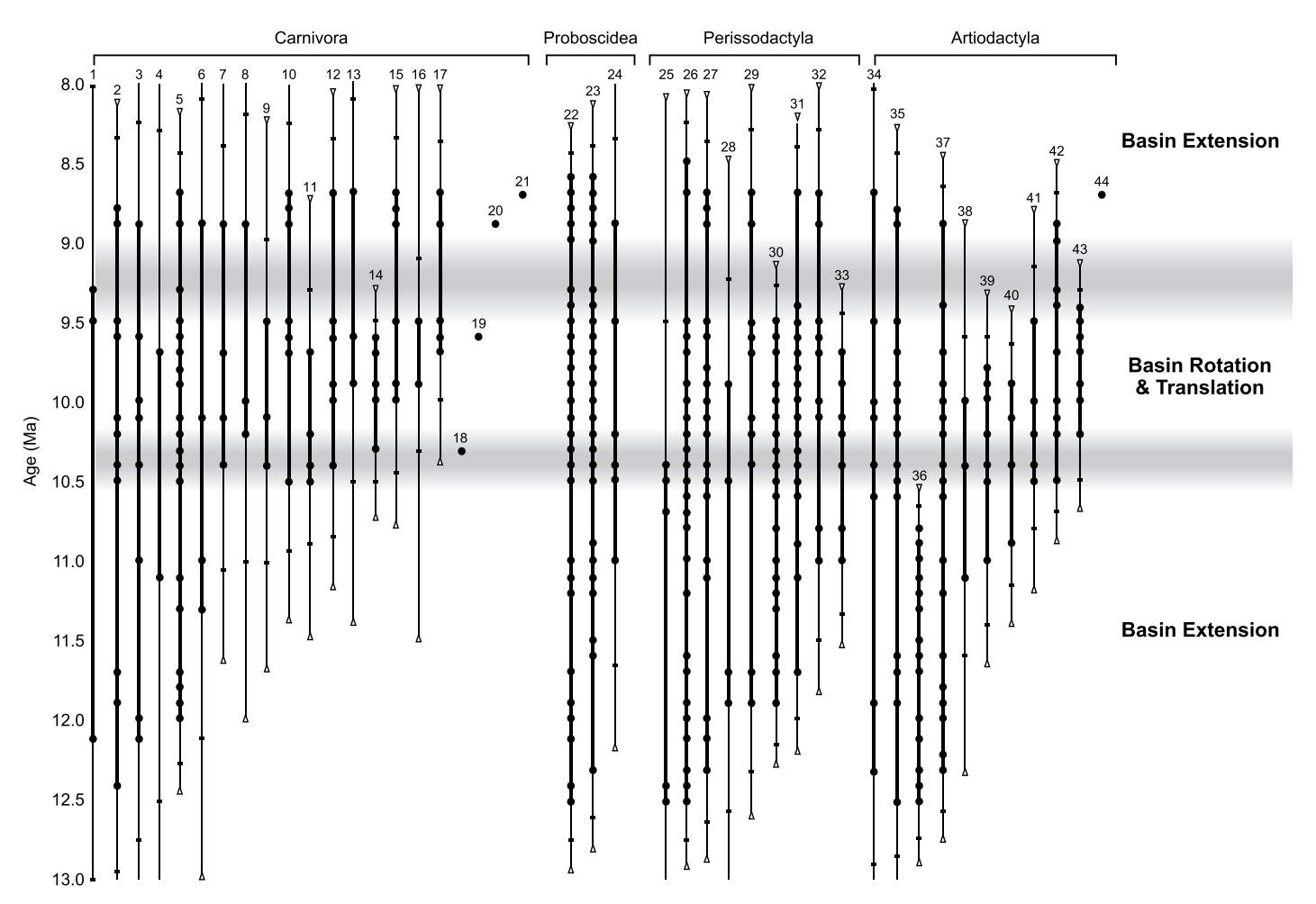


Figure 3. Temporal distribution of large mammals from the Dove Spring Formation. Stratigraphic occurrences of fossil taxa are denoted by black points. Thick vertical lines represent observed residence time with thin vertical lines indicating 80% confidence intervals with endpoints indicated by white triangles. Unbiased point estimates of first and last occurrences are indicated by horizontal tick marks. Tectonic episodes are marked by gray zones to indicate uncertainty in the timing of their initiation. Numbers correspond to taxon names listed in Table A1.

To evaluate change in faunal composition, we used a multinomial likelihood method to compare change between adjacent 200-kyr time intervals. Equation 3 is the log-likelihood (LnL) of the multinomial distribution (Edwards, 1992; Handley et al., 2009; Finarelli and Badgley, 2010). For each time interval of interest (*i*) and its preceding interval, we calculated the proportion of species in each family from the total assemblage and the likelihood of that proportion.

The equation to calculate the log-likelihood of the multinomial distribution is:

$$\operatorname{LnL}(i) = \Sigma_i a_i \ln(p_i), \tag{3}$$

where:

a<sub>j</sub> = count of species in family j, and
p<sub>j</sub> = proportion of total species in interval i assigned to family j.

We compared the maximum likelihood of faunal proportions for each time interval to the maximum likelihood estimate based on the preceding interval by subtracting the latter from the former, to evaluate the difference in log-likelihood values (delta LnL). The results were used to evaluate changes in faunal composition among subsequent time intervals; the magnitude of delta LnL is higher with increasingly divergent proportions among intervals. A delta LnL value of 2.0 is the standard threshold for statistically significant change in maximum-likelihood estimates (Edwards, 1992; Badgley and Finarelli, 2013).

Variations in sampling frequency and preservation contribute to uncertainty in rates of origination and extinction in the fauna, which are based on first and last occurrences of lineages. We used Foote's (2000) estimate of preservation rate to evaluate changes in the quality of the fossil record for comparison with rates of origination and extinction. This estimate of preservation

rate is calculated by comparing the total number of taxa (including range-through taxa) actually observed in a given interval with the estimated number of taxa (including range-through taxa) based on unbiased point estimates of their first and last occurrences. We calculated the preservation rate r(i) for each 200-kyr interval of the fossil record using Foote's (2000) equation:

$$r(i) = -\ln\left(1 - N_{\text{bt, samp}}(i)/N_{\text{bt}}(i)\right), \tag{4}$$

where

 $N_{\text{bt,samp}}(i)$  = number of species observed in the fossil record, including range-through taxa, whose residence time indicates the likelihood of their presence in an interval (i), and

 $N_{\rm bt}(i)=$  estimated number of species in an interval (i), including range-through taxa based on unbiased point estimates of their first and last occurrences.

We compared changes in species richness based on observed and estimated residence times and determined the observed and estimated number of "originations" and "extinctions" that occurred within each time interval. Here, "originations" refer to first appearances and may include endemic speciation events or immigrations, while "extinctions" refer to last appearances, including actual extinctions or emigration of species. Stratigraphic processes, such as changes in sediment availability or depositional environment, may also lead to variable preservation and uncertainty in residence times (Holland, 2016). The majority of species are found elsewhere in the Basin and Range or Great Plains regions before and after their first appearance in the Dove Spring Formation (Tedford et al., 2004; Pagnac, 2009; Whistler et al., 2009; Priego-Vargas et al., 2016).

We used the per capita approach to diversification of Foote (2000). This approach recognizes four categories of occurrences: species confined within a single time interval (singletons), bottom-boundary crossers ( $N_b$ ) with a last occurrence during the focal interval, top-boundary crossers ( $N_t$ ) with a first appearance in the focal interval, and taxa that range through the focal interval and cross both the bottom and top boundaries ( $N_{bt}$ ). We calculated the standing richness and per capita rates of origination p(i) and extinction q(i) for each interval as follows:

$$p(i) = -\ln(N_{bt}(i)/N_t(i)), \tag{5}$$

$$q(i) = -\ln(N_{bt}(i)/N_b(i)), \tag{6}$$

where:

 $N_{\rm bl}(i)$  = range-through taxa,  $N_{\rm t}(i)$  = top-boundary crossers, and  $N_{\rm b}(i)$  = bottom-boundary crossers.

We determined rates of diversification from the per capita origination and extinction rates to evaluate the per capita rate of change in species richness for each interval. Diversification rate d(i) is the net change in species richness, which is expressed as the absolute difference between per capita rates of extinction and origination (Equation 7; Foote, 2000; Badgley and Finarelli, 2013; Domingo et al., 2014). Diversification rate d(i) is expressed as:

$$d(i) = (N_{t}(i) - N_{b}(i))/N_{bt}(i), \tag{7}$$

where

 $N_{\rm bt}(i)$  = range-through taxa,  $N_{\rm t}(i)$  = top-boundary crossers, and  $N_{\rm b}(i)$  = bottom-boundary crossers.

To evaluate the significance of the diversification metrics, we used Microsoft Excel 2016 to generate 1000 bootstrap replicates of the estimated temporal durations of each taxon. Each bootstrapped dataset was generated using a random pull of the 49 large mammal taxa with replacement based on estimated first and last occurrences. For each time interval, we determined confidence intervals of origination rate, extinction rate, and diversification rate as two standard deviations of the mean of the bootstrap distribution. Values of each metric are considered to be statistically significant (nonzero at ~95% confidence) when the confidence intervals on the bootstrap distribution do not include zero (Foote, 2000).

To determine how much variable sampling influenced richness patterns, we conducted shareholder quorum subsampling (SQS) based on the method of Alroy (2010, 2020). This method estimates the number of species that would be found in a subsample of an assemblage with a fixed "coverage," or level of completeness, based on the proportion of individuals in the population. Each taxon is considered "covered" when it is represented by at least one specimen in a dataset. SQS allows for less biased comparison of species richness from time intervals with varying sample sizes. We used PAST: Paleontological Statistics version 4.13 (Hammer et al., 2001) to calculate the mean number of species in each time interval based on 1000 iterations of the observed fossil record for each of three target coverage levels or proportions (0.4, 0.6, and 0.8) and compared our results to observed species richness. If sampling were the primary driver of species richness, we would expect the SQS species richness curve to be relatively flat through all time intervals. However, if variability in the SQS species richness curve corresponds to the observed species richness pattern, it would indicate that the observed richness patterns actually occurred. Our calculations use an assumption of convenience that every fossil specimen represents an individual. Taphonomic data and bone-element analysis would be necessary to further refine these estimates but are beyond the scope of this study.

### RESULTS

In this section, we first present the stratigraphic and geochronologic framework of the Dove Spring Formation. We then describe the biochronology of large mammals and patterns of change in faunal composition. Finally, we compare the patterns of origination and extinction based on estimated residence times to the tectonic history of the El Paso Basin. To mitigate the influence of edge effects on the fossil record, we excluded the first and last two 200-kyr intervals from our analyses.

## Stratigraphic and Geochronologic Framework

Our new stratigraphic sections provide context for the spatial distribution of fossil localities and their stratigraphic placement within the updated chronology of the Dove Spring Formation, with a stratigraphic resolution of  $\sim$ 25–50 m and a temporal resolution of 200 k.y. (Fig. 2). The chronostratigraphy for most of the study interval is well resolved based on radiometric ash dates using current decay constants and correlation with the geomagnetic time scale. Based on a new tephrochronologic correlation to the marine Monterey Formation from Knott et al. (2022; Table 2), we revised the age of the top of the study interval to 8.5 Ma and adjusted species' temporal ranges accordingly. The majority of revised ash dates fall within their original uncertainty estimates ( $\pm 0.03$  m.y.; Table 2).

We recorded lithological variation in the lower 600 m of the formation, adding information to a sparsely documented section of the study interval (Fig. 2). We also correlated dated ash layers to additional outcrops throughout the basin based on stratigraphically adjacent and laterally continuous units observed in the field. The lithological and geochronological changes that are most relevant to our study occur in the upper half of the Dove Spring Formation due to their association with boundaries between tectonic episodes. Sediments in the upper half of the formation begin at 900 m in the W92B section (Fig. 2), with a thick interval of fine- to medium-grained sandstones interbedded with mudstones extending upward to 1400 m (ca. 10.5-9.0 Ma; Fig. 2). Sandstones then coarsen significantly and include an increasing proportion of granitic clasts above 1400 m (9.0 Ma), which signifies a change in source area from the El Paso Mountains to the Sierra Nevada Range (Loomis and Burbank, 1988).

The average sediment accumulation rate for the entire Dove Spring Formation is 383 m/m.y. The rate varies between 100 m/m.y. and 650 m/m.y. over time spans of 0.3 m.y. to 0.5 m.y. for the first 2 m.y. of deposition, when a series of sandstones and silty sandstones sourced from the El Paso Mountains was deposited in the basin (Fig. 4A). A moderate peak of 650 m/m.y. occurs at 11.8 Ma, driven in part by the deposition of tuff breccia associated with regional volcanism, and conglomerates and sandstones from the El Paso Mountains. A moderate peak of 893 m/m.y. occurs at 10.3 Ma following at least 1 m.y. of very slow accumulation of similar sediments. Basin rotation and translation began concurrently with this peak and preceded another long period of slow sedi-

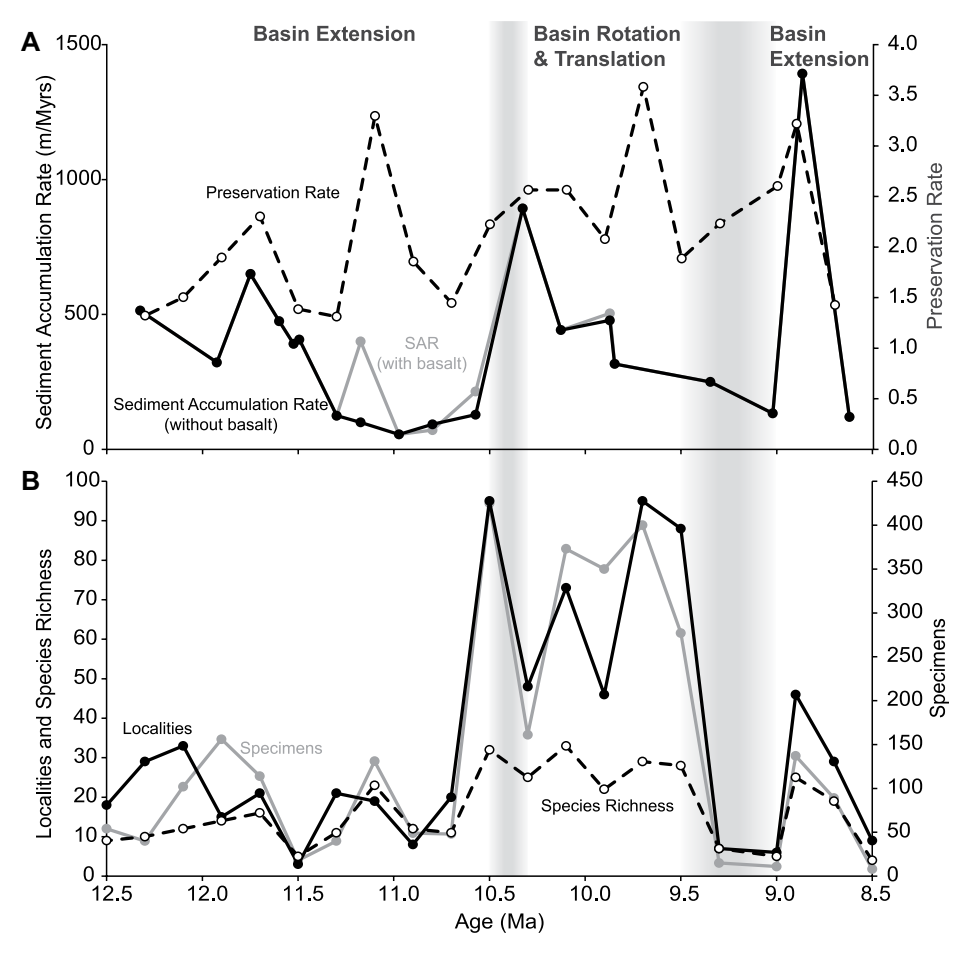


Figure 4. (A) Sediment accumulation rate (SAR) and preservation rate for the El Paso Basin. We removed a pair of basalt flows from our calculations to more accurately represent the basin's mode of sediment accumulation. As a result, SAR was lower near  $11.0\,\mathrm{Ma}$ , and a moderate peak is no longer present. (B) Large mammal (>1 kg) fossil specimens recovered from the Dove Spring Formation, number of localities, and species richness are based on raw observed occurrence data, excluding range-through taxa. Specimens recovered from the base of the formation are represented by points at  $12.5\,\mathrm{Ma}$ . Tectonic episodes that began during the study interval are marked with gray zones to indicate uncertainty in the timing of their initiation.

ment accumulation. Basin extension resumed no later than 9.3 Ma, shortly before coarse, granitic clasts from the Sierra Nevada were deposited during a final peak of 1300 m/m.y. at 8.9 Ma.

### **Biochronology and Faunal Composition**

Fossils recovered from the Dove Spring Formation are the basis for initial interpretations of

changes in species richness and the quality of the fossil record (Figs. 3 and 4). The number of largemammal specimens per interval closely follows the number of localities per interval (r = 0.90, p < 0.05). Two exceptions occur prior to 11.0 Ma (Fig. 4B). At 12.0 Ma and 11.1 Ma, the number of specimens increases sharply despite decreasing locality frequency. The interval between 10.5 Ma and 9.5 Ma contains the greatest number of localities and specimens, peaking at 9.5 Ma. A significant dip in both localities and specimens occurs at 9.3 Ma, before rising again at 8.9 Ma. The observed species richness of large mammals per time interval generally follows the same pattern as the number of localities (r = 0.88, p < 0.05) and specimens (r = 0.89, p < 0.05). A steady increase from nine species at the base of the formation reaches 33 species by 10.1 Ma. Species richness is highest between 10.5 Ma and 9.5 Ma, which is consistent with the highest numbers of localities and specimens and suggests that species richness reflects sampling intensity. Estimates of standing richness follow a pattern similar to that of the observed standing richness (Fig. 5). Preservation rate is moderate throughout most of the formation, although spikes occur at 11.1 Ma, 9.7 Ma, and 8.9 Ma (Fig. 4A).

Seventeen species occur within the first 200 k.y. of deposition in the Dove Spring Formation (Figs. 3 and 5). Merycoidodontids and antilocaprids are present at the base of the formation and maintain their species richness throughout the study interval, with the exception of a dip in antilocaprid species richness at 10.7 Ma (Fig. 6A). Camelids exhibit a similar pattern but gain additional species between 10.5 Ma and 9.5 Ma. Equids are present at the base of the formation and steadily gain species until reaching peak richness (seven species) at 11.1 Ma, after which they maintain high richness until 9.5 Ma. Tayassuids appear at 11.1 Ma and persist until 9.9 Ma. Gomphotheriids appear at the base of the formation and persist until 8.7 Ma, while amebelodontids appear at 11.1 Ma and disappear from the formation after 8.9 Ma.

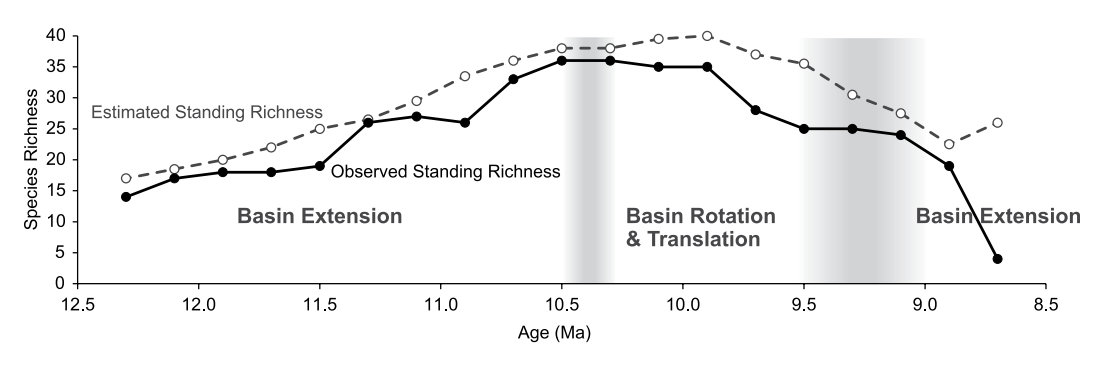


Figure 5. Standing richness of the Dove Spring Formation, excluding singletons due to their high dependence on preservation, resulting in a maximum species richness of 40, which is lower than the raw count (45). These plots incorporate rangethrough taxa and provide a better estimate of actual richness than the raw occurrence counts in Figure 4B. Both the observed and estimated fossil records follow a unimodal pattern.

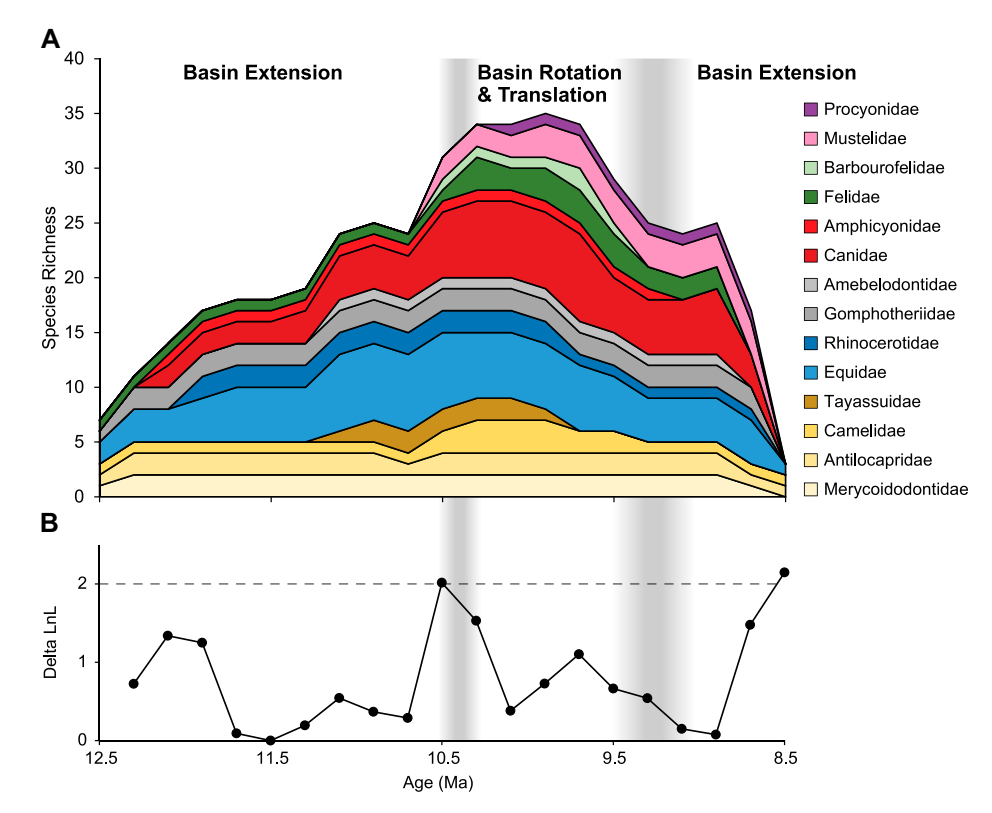


Figure 6. Taxonomic composition of large mammals in the Dove Spring Formation through time, including singletons. (A) Stacked richness of family-level species richness. (B) Change in log-likelihood ratios (delta LnL) of large-mammal assemblage composition. Values of 2.0 or greater indicate statistically significant change in faunal composition for a given time interval compared to the previous interval. The 10.5 Ma peak is driven by the first appearances of Barbourofelidae and Mustelidae, as well as additional species of Antilocapridae, Camelidae, and Canidae. The 8.5 Ma peak is the result of species loss in the Canidae, Equidae, Gomphotheriidae, and Mustelidae. An additional peak at 12.1 Ma was driven by the first appearances of Amphicyonidae, Canidae, and Rhinocerotidae, but the delta LnL values of this peak do not reach the threshold of statistical significance.

As in most assemblages, carnivores are considerably rarer than herbivorous taxa. Felids are present at the base of the formation, but remain rare until 10.3 Ma, after which they maintain higher richness until 8.7 Ma. Barbourofelids are rare and only found during the most wellsampled interval, between 10.5 Ma and 9.5 Ma. Canids are consistently the most species-rich family of carnivores after their first appearance at 12.1 Ma, and steadily gain species at 11.1 Ma, reaching their maximum richness at 9.7 Ma. Procyonids are represented by a single species that is present from 10.1 Ma until 8.7 Ma. Smaller carnivores are not found prior to 10.5 Ma, when two species of mustelids appear and persist through the top of the formation.

Statistically significant (nonzero at  $\sim$ 95% confidence) changes in faunal composition occurred in two intervals of time, according to the change in log likelihoods (delta LnL; Fig. 6B). Change at 10.5 Ma was driven by the

largest influx of new species, including the first appearances of Barbourofelidae and Mustelidae, as well as additional species of Antilocapridae, Camelidae, and Canidae. Change at 8.5 Ma was the result of species loss in the Canidae, Equidae, Gomphotheriidae, and Mustelidae. Following 10.5 Ma, the only additional species to appear were a canid (Metalopex macconnelli), a felid (Pseudaelurus sp.), and four singletons (Barbourofelis whitfordi, Carpocyon webbi, cf. Illingoceros sp., and an unidentified member of the Vulpinae). An additional moderate peak of change in faunal composition occurred at 12.1 Ma and was driven by the first appearance of species of Amphicyonidae, Canidae, and Rhinocerotidae, as well as an additional species of Equidae. While this peak does not reach the threshold of statistical significance, it is notable for coinciding with a low preservation rate and is unlikely to be the result of an edge effect due to its temporal placement 400 k.y. into the formation.

### Diversification

Our analyses of the species richness and diversification of large mammals are based on estimated residence times (Figs. 3 and 5). Per capita origination and extinction rates depict the proportion of species appearing or disappearing from the study interval, standardized by rangethrough taxa (Fig. 7). Per capita origination rates were moderate and reached two statistically significant peaks at 11.7 Ma and 11.1 Ma, after which a steady decline began (Fig. 7B). Per capita extinction rates exhibit a gradual increase between 9.9 Ma and 9.3 Ma, before a sharp decrease at 9.1 Ma. Statistically significant per capita extinction rates are present between 9.7 Ma and 9.3 Ma.

We found weak correlations (p < 0.05)between preservation rate and per capita origination rate (r = -0.18), per capita extinction rate (r = 0.17), and species richness (r = 0.55). Peaks in preservation rate that coincide with peaks in per capita origination rate indicate that new species are the result of increased preservation. However, peaks in per capita origination rate that occur regardless of preservation rate indicate faunal changes that are not driven by preservation. The 11.7 Ma and 11.1 Ma peaks in per capita origination coincide with peaks in preservation, although the higher preservation rate at 11.1 Ma does not result in a greater per capita origination rate. The earliest peak in per capita extinction rate at 9.7 Ma coincides with a peak in preservation rate, while the following two extinction rate peaks coincide with much lower preservation rates. A sharp decrease in per capita extinction rate coincides with a final peak in preservation rate at 8.9 Ma.

The per capita diversification rate is positive until 9.7 Ma and follows the same patterns as per capita origination and extinction rates, with two positive peaks at 11.7 Ma and 11.1 Ma and a series of three negative values between 9.7 Ma and 9.3 Ma (Fig. 7C). Two extended time intervals exhibit diversification rates that coincide with episodes of tectonic extension: the internal peaks of per capita origination at 11.7 Ma and 11.1 Ma represent a trend of origination in the lower half of the formation (12.5-10.5 Ma) and occur during a tectonic episode of extension that began in the middle Miocene and continued during the deposition of the Dove Spring Formation. The upper half of the formation exhibits increasing extinction rates following the onset of basin rotation and translation. The sharp decrease in extinction rate near the top of the formation coincides with peaks in preservation and sediment accumulation rates at 8.9 Ma.

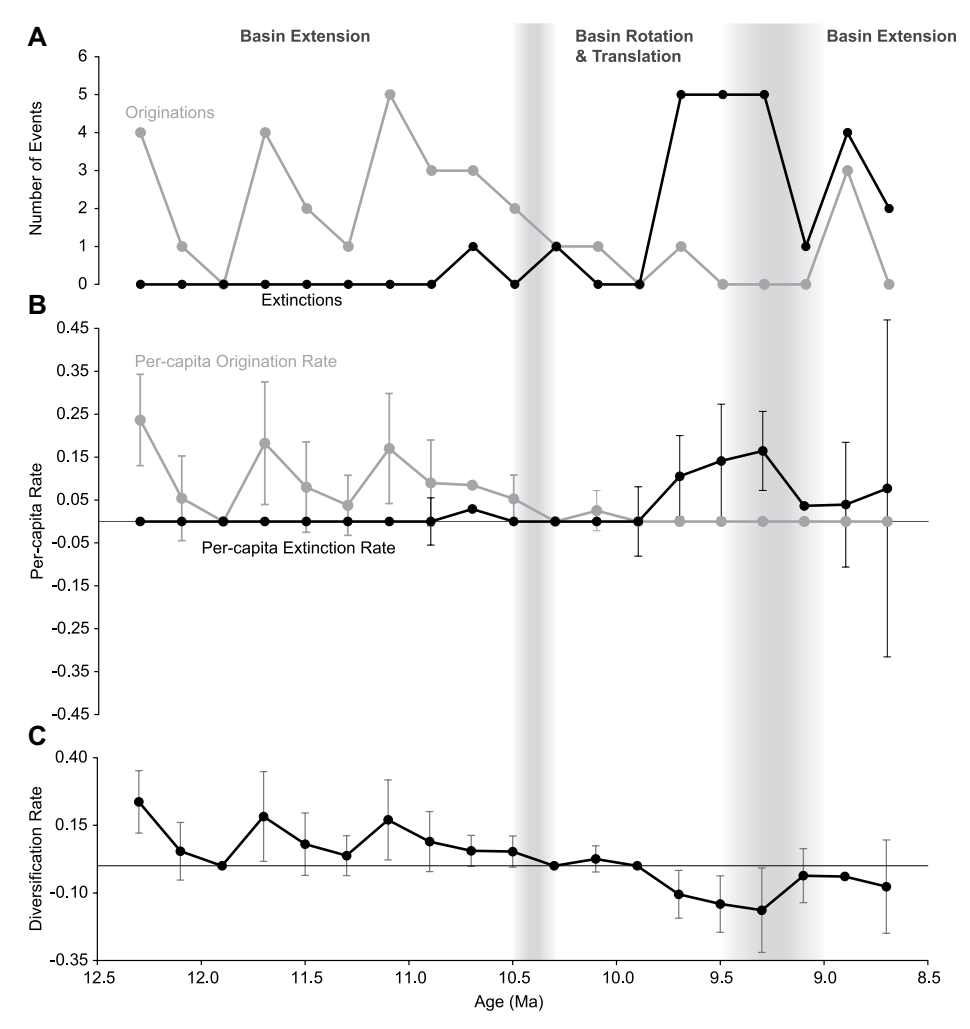


Figure 7. Diversification of large mammals based on estimated residence times. (A) Originations (first appearances) and extinctions (last appearances) based on bottom- and top-boundary crossing taxa. (B) Per capita origination and extinction rates. (C) Per capita diversification rate. Tectonic episodes of basin rotation followed by extension are marked with gray zones to indicate uncertainty in the timing of their initiation. Confidence intervals are based on 1000 bootstrap replicates of the dataset and are considered statistically significant (nonzero with  $\sim\!95\,\%$  confidence) when they do not intersect with zero (marked with thin horizontal lines).

### DISCUSSION

We used estimated residence times to determine the number and per capita rates of origination and extinction to test whether changes in species richness and faunal composition could have been influenced by changes in tectonic history. The three tectonic episodes recorded in the Dove Spring Formation each correspond with a different phase of faunal change, which we describe below.

North-south extension that began in the middle Miocene was the dominant tectonic process early in the formation's history (12.5–10.5 Ma). During this phase of extension, the basin grew in area and subsidence increased (Loomis and Burbank, 1988; Gawthorpe and Leeder, 2000).

The deposition of fine-grained fluvial and lacustrine sediments suggests that drainage channels had relatively gentle slopes and for a time fed a lake in the northern part of the basin (Gawthorpe and Leeder, 2000). The lowest sediment accumulation rates occur at 11.0 Ma and indicate slow changes in subsidence rates or continued basin growth. Peaks in per capita origination occurred at 11.7 Ma and 11.1 Ma, suggesting that extension opened corridors for an influx of species from outside the basin. Positive origination and diversification rates are often correlated with area (Kisel et al., 2011). A greater area supports larger population sizes and also promotes increased habitat diversity, with the potential to generate environmental gradients that allow for a higher number of species to coexist. Here, the

gradual accumulation of species prior to 10.0 Ma is driven, in part, by the long-term generation of additional habitat space as the basin grew in area. High delta LnL values at 12.1 Ma and 11.9 Ma indicate measurable changes in faunal composition that are driven by an additional equid species and the first appearances of amphicyonids, canids, and rhinocerotids. With the exception of amphicyonids, these taxa persist to the top of the formation.

Rotation and translation of the El Paso Basin along the Garlock fault began at 10.5 Ma, interrupting the long episode of basin growth. The basin's geometry and relationships to its sediment sources in the El Paso Mountains were altered, triggering changes to drainage patterns and likely the availability of water and vegetation. A peak in subsidence coincided with the onset of shear movement and then gradually decreased until ca. 9.0 Ma. While environmental conditions during this episode were conducive to preservation, consistently yielding the highest species richness within the formation, extinction became the dominant pattern of faunal change (Figs. 4A and 7B). The highest preservation rate occurred at 9.7 Ma, coinciding with a low peak of change in faunal composition due to apparent species loss across multiple families, but species richness remained elevated until the start of the next tectonic interval.

East-west extension beginning near 9.5 Ma increased the distance between the depositional center of the basin and its original sedimentsource area. This episode represents a new stage of basin extension that generated the coarser sediments with a source in the Sierra Nevada. The resulting depositional environments were more likely to preserve fossils early in this episode, as indicated by an increasing preservation rate, but localities, specimens, and species richness reached their lowest frequencies during the early stages of this extension (Fig. 4A). Per capita extinction rates were constant through the end of the study interval (Fig. 7B). Negative diversification rates coincide with the apparent disappearance of six species from the basin's fossil record, and singletons are the only new species that occurred after the onset of extension.

While a positive correlation exists between species richness and the number of localities (Fig. 4), there is also evidence for changes in richness and faunal composition that cannot be solely attributed to sampling. High per capita origination rates in the lower half of the formation (11.7 Ma and 11.1 Ma) are coupled with low numbers of localities compared to the well-sampled middle portion and high preservation rates. The correlation among these three patterns suggests that preservation during the early extensional episode had a strong influence on species richness. However, several taxa made their first

appearances between 11.7 Ma and 11.1 Ma and persisted throughout the rest of the formation despite variable preservation (Figs. 4 and 6).

The pattern of rare taxa with long residence times occurs again in the upper half of the formation, which is dominated by high rates of extinction and exhibits a greater magnitude of faunal change. The greatest change in faunal composition occurred at 10.5 Ma and was driven by additional species of Antilocapridae, Camelidae, and several carnivores (Fig. 6). The majority of carnivore species that appeared during this interval persisted through the top of the formation, which indicates that their presence was not entirely tied to sampling. The highest species richness (40) occurred at 9.9 Ma, during an interval when preservation rate was decreasing (Figs. 4A, 5, and 7B). Despite thorough sampling efforts and a spike in preservation rate at 9.7 Ma, few additional species are recovered high in the formation (Figs. 4 and 6).

An important point to consider is whether the patterns of faunal change in the formation represent real processes or result from fluctuations in sampling. If fossil productivity were the primary control on the record of faunal change, we would expect strong correlations among preservation, sampling, and processes of faunal change. However, throughout the formation, we calculated weak relationships between preservation and all other variables. The number of range-through taxa that persist through multiple time intervals is consistently high, and the average residence time for large-mammal species was 2.1 m.y. The

appearance of rare taxa in intervals with low preservation potential and only few localities is contrary to the expectations of poor sampling (we would expect the common species to persist). While preservation is always a factor when examining the fossil record, our results indicate that the patterns of faunal change within the Dove Spring Formation are not entirely tied to the quality of the fossil record.

SQS analyses demonstrate that patterns of faunal change and species richness are detectable in the Dove Spring Formation even at low rates of sampling (Fig. 8). Despite the presence of several highly dominant taxa (notably Antilocapridae, Equidae, and Camelidae) and variable preservation rates, SQS species richness exhibits variability similar to that of observed species richness throughout the formation. The relationship between SQS and observed richness indicates that while sampling played a role in the observed fossil record, our analyses captured real patterns of faunal change and species richness.

Additional data about the history of depositional environments are needed to evaluate the influence of preservation on species richness and the composition of large-mammal assemblages. Changes in the dominant lithologies from coarse-grained breccia and sandstones in the lower part of the formation, to fine- to medium-grained silty sandstones in the middle, to coarse conglomerates in the upper part track changes in the preservation potential of the basin (Fig. 2). Facies analysis of depositional environments provides the data necessary to investigate

potential ecological causes for faunal change, such as changes in vegetation resources, precipitation amount, and paleotemperature. The additional environmental information, in combination with this analysis of taxonomic richness and the timing of tectonic episodes, will enable us to test two hypotheses regarding the correlations among the physical environment and changes in the mammalian faunas of the basin. One hypothesis is that the tectonic episodes altered the preservation potential of sediments and depositional environments. In this scenario, changes in fossil productivity would occur in the

tectonic and sedimentological controls on fossil

preservation. Environmental data from isotopes

of mammalian tooth enamel are indicators of

absence of significant ecological change; mammalian species would not exhibit marked changes in feeding ecology or body size, and the community composition would change little throughout the section, regardless of depositional environment. Changes in depositional environments can be identified through facies analysis and correlated with the timing of tectonic activity to evaluate whether changes in preservation affect the fossil record of the Dove Spring Formation.

An alternative hypothesis is that tectonic influences on basin topography contributed to significant change in the environments present within the Dove Spring Formation. An independent record of change in climate or vegetation would provide evidence for testing this hypothesis. Under this scenario, we would expect to observe significant variation in ecological diversity within the mammalian fauna that coincides with the timing of tectonically driven changes in depositional setting and climate. Mammalian body size is correlated with ecological characteristics such as diet, population density and growth rate, home range size, and behavioral adaptations (Damuth and MacFadden, 1990; Eisenberg, 1990; Janis et al., 2002). Changes in the range of ungulate body sizes that coincide with the basin's tectonic history would support the hypothesis that changes in habitat affected ecological variables. The stable isotopic ratios of carbon in herbivore teeth also document the composition of vegetation (Quade et al., 1992; Koch et al., 1994; Cerling et al., 1997). Significant change in isotopic values that correlate with tectonic episodes would support this second hypothesis.

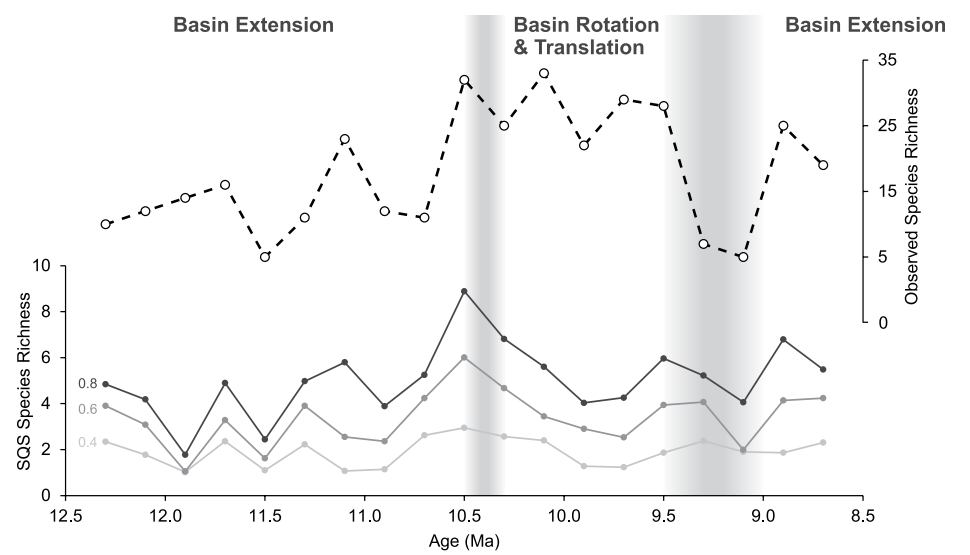


Figure 8. Shareholder quorum subsampling (SQS) estimates of species richness (lower lines) compared to observed species richness (upper dashed line). Each SQS richness curve represents the mean value of 1000 iterations for three coverage levels (0.4, 0.6, and 0.8). The correlation between the two measures indicates that changes in species richness are detectable even with low sampling effort.

### CONCLUSION

Study sites like the El Paso Basin are part of a growing record of basins that are providing insight into the interactions between changing topography and mammalian evolution (Badgley and Finarelli, 2013; Badgley et al., 2017; Loughney and Badgley, 2017; Smiley et al., 2018). The Dove Spring Formation is a record of mammalian faunas preserved in the sediments of a basin that developed during the end of the Middle Miocene Climatic Transition. We reviewed its geochronology using updated decay constants and newly measured stratigraphic sections to place fossil localities within a temporal and stratigraphic framework for analysis and to support additional paleoecological research.

We identified two phases of change in taxonomic richness: high species accumulation and long residence times low in the formation, and steady species loss in the upper portion. These patterns are primarily influenced by fossil productivity, but the presence of rare taxa that persisted throughout the formation provides evidence that some faunal changes cannot be explained by sampling alone. The study interval includes three major tectonic episodes that altered the basin's geometry and topography. Basin extension in the lower part of the section was associated with an increase in basin area, high per capita origination rates, and minor changes in faunal composition. At 10.5 Ma, the basin underwent a period of rotation and translation away from the El Paso Mountains, disrupting existing drainages and likely affecting connectivity to the surrounding region. High numbers of specimens, localities, and species accompanied the highest magnitude of change in faunal composition at 10.5 Ma. Preservation rates peaked twice in the upper half of the formation, but the per capita extinction rate became the dominant expression of faunal change. Extinction rates continued to increase until 9.3 Ma, as basin extension resumed and coarse sediments from the Sierra Nevada became prevalent. New drainage networks began to form and changed the preservation potential of sediments or generated new environmental settings, either way leading to the apparent or actual disappearance of most species from the El Paso Basin's fossil record.

Distinct episodes of tectonic history coincided with the timing of changes in faunal patterns, which suggests a link between tectonic processes and the basin's mammalian community. The timeline of tectonic and faunal changes in this study provides the framework for further testing of the nature of this link through studies of preservation potential, depositional environments, and vegetation history.

### ACKNOWLEDGMENTS

We received funding for this research from the Rackham Graduate School and the Department of Earth and Environmental Sciences at the University of Michigan. We acknowledge support from the National Science Foundation, Integrated Earth Systems Program award #1813996 to C. Badgley. We thank Xiaoming Wang, Juliet Hook, Sam McCleod, and Vanessa Rhue of the Natural History Museum of Los

TABLE A1. TAXON NAMES CORRESPONDING TO NUMBERS IN FIGURE 3

Species no.	Order	Family	Species name
1	Carnivora	Amphicyonidae	Ischyrocyon mohavensis
2	Carnivora	Felidae	Felidae
3	Carnivora	Canidae	Epicyon saevus
4	Carnivora	Canidae	Carpocyon robustus
5 6	Carnivora	Canidae	Canidae
6	Carnivora	Canidae	Leptocyon vafer
7	Carnivora	Canidae	Borophagus littoralis
8	Carnivora	Felidae	Homotherium sp.
9	Carnivora	Barbourofelidae	Barbourofelis sp.
10	Carnivora	Mustelidae	Martes buwaldi
11	Carnivora	Canidae	Epicyon haydeni
12	Carnivora	Mustelidae	Mustelidae
13	Carnivora	Mustelidae	Martinogale faulli
14	Carnivora	Canidae	Epicyon sp.
15	Carnivora	Procyonidae	Bassariscus sp.
16	Carnivora	Felidae	Pseudaelurus sp.
17	Carnivora	Canidae	Metalopex macconnelli
18	Carnivora	Felidae	<i>Nimravides</i> sp.
19	Carnivora	Barbourofelidae	Barbourofelis whitfordi
20	Carnivora	Canidae	Carpocyon webbi
21	Carnivora	Canidae	Vulpinae
22	Proboscidea	Gomphotheriidae	Gomphotheriidae
23	Proboscidea	Gomphotheriidae	Gomphotherium sp.
24	Proboscidea	Amebelodontidae	Amebelodon burnhami
25	Perissodactyla	Equidae	Megahippus sp.
26	Perissodactyla	Equidae	Pliohippus tantalus
27	Perissodactyla	Equidae	Hipparion sp.
28	Perissodactyla	Rhinocerotidae	Aphelops sp.
29	Perissodactyla	Rhinocerotidae	Rhinocerotidae
30	Perissodactyla	Equidae	Cormohipparion sp.
31	Perissodactyla	Equidae	Hipparion forcei
32	Perissodactyla	Equidae	"Dinohippus" leardi
33	Perissodactyla	Equidae	Hipparion tehonense
34	Artiodactyla	Merycoidodontidae	Merycoidodontidae
35	Artiodactyla	Merycoidodontidae	Merychyus major
36	Artiodactyla	Antilocapridae	Paracosoryx furlongi
37	Artiodactyla	Antilocapridae	Cosoroyx sp.
38	Artiodactyla	Tayassuidae	Prosthennops sp.
39	Artiodactyla	Camelidae	Procamelus sp.
40	Artiodactyla	Tayassuidae	Tayassuidae <sup>.</sup>
41	Artiodactyla	Camelidae	Aepýcamelus sp.
42	Artiodactyla	Antilocapridae	Plioceros sp.
43	Artiodactyla	Camelidae	Megatylopus sp.
44	Artiodactyla	Antilocapridae	cf. <i>Illingoceros</i> sp.

Angeles County for granting us access to the vertebrate specimen database and for assistance in the field. We thank Dave Whistler for generously donating his original field notes and for conversations that led to a greater understanding of the Dove Spring Formation. Steve Holland, Ross Secord, and an anonymous reviewer provided helpful comments on the manuscript.

### APPENDIX

See Table A1.

### REFERENCES CITED

Alroy, J., 2010, Fair sampling of taxonomic richness and unbiased estimation of origination and extinction rates, in Alroy, J., and Hunt, G., eds., Quantitative Methods in Paleobiology: The Paleontological Society Papers, v. 16, p. 55–80, https://doi.org/10.1017 /S1089332600001819.

Alroy, J., 2020, On four measures of taxonomic richness: Paleobiology, v. 46, no. 2, p. 158–175, https://doi.org/10.1017/pab.2019.40.

Andrew, J.E., Walker, J.D., and Monastero, F.C., 2015, Evolution of the central Garlock fault zone, California: A major sinistral fault embedded in a dextral plate margin: Geological Society of America Bulletin, v. 127, p. 227–249, https://doi.org/10.1130/B31027.1.

Asher, R.J., and Helgen, K.M., 2010, Nomenclature and placental mammal phylogeny: BMC Evolutionary Biology, v. 10, no. 102, p. 1–9.

Axelrod, D., 1977, Outline history of California vegetation, in Barbour, M., and Major, J., eds., Terrestrial Vegetation of California: New York, John Wiley & Sons, p. 139–194.

Badgley, C., and Finarelli, J.A., 2013, Diversity dynamics of mammals in relation to tectonic and climatic history: Comparison of three Neogene records from North America: Paleobiology, v. 39, no. 3, p. 373–399, https://doi.org/10.1666/12024.

Badgley, C., Smiley, T.M., Terry, R., Davis, E.B., DeSantis, L.R.G., Fox, D.L., Hopkins, S.S.B., Jezkova, T., Matocq, M.D., Matzke, N., McGuire, J.L., Mulch, A., Riddle, B.R., Roth, V.L., Samuels, J.X., Stromberg, C.A.E., and Yanites, B.J., 2017, Biodiversity and topographic complexity: Modern and geohistorical perspectives: Trends in Ecology & Evolution, v. 32, no. 3, p. 211–226, https://doi.org/10.1016/j.tree.2016.12.010.

Bahadori, A., Holt, W.E., and Rasbury, E.T., 2018, Reconstruction modeling of crustal thickness of western North America since 36 Ma: Geosphere, v. 14, p. 1207–1231, https://doi.org/10.1130/GES01604.1.

Begemann, F., Ludwig, K.R., Lugmair, G.W., Min, K., Nyquist, L.E., Pratchett, P.J., Renne, P.R., Shih, C.-Y., Villa, I.M., and Walker, R.J., 2001, Call for an improved set of decay constants for geochronological use: Geochimica et Cosmochimica Acta, v. 65, no. 1, p. 111–121, https://doi.org/10.1016/S0016-7037(00)00512-3.

Bonnichsen, B., Leeman, W.P., Honjo, N., McIntosh, W.C., and Godchaux, M.M., 2008, Miocene silicic volcanism in southwestern Idaho: Geochronology, geochemistry, and evolution of the central Snake River Plain: Bulletin of Volcanology, v. 70, no. 3, p. 315–342, https://doi.org /10.1007/s00445-007-0141-6.

Burbank, D.W., and Anderson, R.S., 2012, Tectonic Geomorphology: Chichester, UK, Wiley-Blackwell, 472 p.

Camp, V.E., Pierce, K.L., and Morgan, L.A., 2015, Yellowstone plume trigger for Basin and Range extension, and coeval emplacement of the Nevada–Columbia Basin magmatic belt: Geosphere, v. 11, p. 203–225, https:// doi.org/10.1130/GES01051.1.

Carter, J., Ickert, R.B., Mark, D.F., Tremblay, M.M., Cresswell, A.J., and Sanderson, D.C.W., 2020, Production of <sup>40</sup>Ar by an overlooked mode of <sup>40</sup>K decay with implications for K-Ar geochronology: Geochronol-

- ogy, v. 2, no. 2, p. 355–365, https://doi.org/10.5194/gchron-2-355-2020.
- Cerling, T.E., Harris, J.M., Ambrose, S.H., Leakey, M.G., and Solounias, N., 1997, Dietary and environmental reconstruction with stable isotope analyses of herbivore tooth enamel from the Miocene locality of Fort Ternan, Kenya: Journal of Human Evolution, v. 33, p. 635–650, https://doi.org/10.1006/jhev.1997.0151.
- Chamberlain, C.P., Winnick, M.J., Mix, H.T., Chamberlain, S.D., and Maher, K., 2014, The impact of neogene grassland expansion and aridification on the isotopic composition of continental precipitation: Global Biogeochemical Cycles, v. 28, p. 992–1004, https://doi.org /10.1002/2014GB004822.
- Cox, B.F., and Diggles, M.F., 1986, Geologic map of the El Paso Mountains Wilderness Study Area, Kern County, California: U.S. Geological Survey Miscellaneous Field Studies Map 1827, 1 plate, https://doi.org/10 .3133/mf1827.
- Crowley, B.E., Koch, P.L., and Davis, E.B., 2008, Stable isotope constraints on the elevation history of the Sierra Nevada Mountains, California: Geological Society of America Bulletin, v. 120, p. 588–598, https://doi.org/10.1130/B26254.1.
- Damuth, J., and MacFadden, B.J., 1990, Body Size in Mammalian Paleobiology: Estimation and Biological Implications: Cambridge, UK, Cambridge University Press, 397 p.
- Dibblee, T.W., 1967, Areal geology of the western Mojave Desert California: U.S. Geological Survey Professional Paper 522, https://doi.org/10.3133/pp522.
- Dickinson, W.R., 2002, The Basin and Range Province as a composite extensional domain: International Geology Review, v. 44, p. 1–38, https://doi.org/10.2747/0020-6814.44.1.1.
- Dixon, T.H., and Xie, S., 2018, A kinematic model for the evolution of the Eastern California Shear Zone and Garlock Fault, Mojave Desert, California: Earth and Planetary Science Letters, v. 494, p. 60–68, https://doi .org/10.1016/j.epsl.2018.04.050.
- Domingo, M.S., Badgley, C., Azanza, B., DeMiguel, D., and Alberdi, M.T., 2014, Diversification of mammals from the Miocene of Spain: Paleobiology, v. 40, no. 2, p. 197–221, https://doi.org/10.1666/13043.
- Edwards, A.W.F., 1992, Likelihood: Baltimore, Maryland, Johns Hopkins University Press, https://doi.org/10 .56021/9780801844454.
- Eisenberg, J.F., 1990, The behavioral/ecological significance of body size in the Mammalia, *in* Damuth, J., and MacFadden, B.J., eds., Body Size in Mammalian Paleobiology: Estimation and Biological Implications: Cambridge, UK, Cambridge University Press, p. 25–37.
- Eronen, J.T., Janis, C.M., Chamberlain, C.P., and Mulch, A., 2015, Mountain uplift explains differences in Palaeogene patterns of mammalian evolution and extinction between North America and Europe: Proceedings of the Royal Society B: Biological Sciences, v. 282.
- Evernden, J.F., Savage, D.E., Curtis, G.H., and James, G.T., 1964, Potassium-argon dates and the Cenozoic mammalian chronology of North America: American Journal of Science, v. 262, p. 145–198, https://doi.org/10 .2475/ajs.262.2.145.
- Faulds, J.E., and Henry, C.D., 2008, Tectonic influences on the spatial and temporal evolution of the Walker Lane: An incipient transform fault along the evolving Pacific— North American plate boundary: Arizona Geological Society Digest, v. 22, p. 437–470.
- Finarelli, J.A., and Badgley, C., 2010, Diversity dynamics of Miocene mammals in relation to the history of tectonism and climate: Proceedings of the Royal Society B: Biological Sciences, v. 277, p. 2721–2726, https://doi. org/10.1098/rspb.2010.0348.
- Flower, B.P., and Kennett, J.P., 1993, Relations between Monterey Formation deposition and middle Miocene global cooling: Naples Beach section, California: Geology, v. 21, p. 877–880, https://doi.org/10.1130 /0091-7613(1993)021<0877:RBMFDA>2.3.CO;2.
- Foote, M., 2000, Origination and extinction components of taxonomic diversity: General problems: Paleobiology, v. 26, p. 74–102, https://doi.org/10.1666/0094-8373(2000)26[74:OAECOT]2.0.CO;2.

- Frigola, A., Prange, M., and Schulz, M., 2018, Boundary conditions for the Middle Miocene Climate Transition (MMCT v1.0): Geoscientific Model Development, v. 11, p. 1607–1626, https://doi.org/10.5194/gmd-11 1607-2018
- Gawthorpe, R.L., and Leeder, M.R., 2000, Tectono-sedimentary evolution of active extensional basins: Basin Research, v. 12, p. 195–218, https://doi.org/10.1111/j.1365-2117.2000.00121.x.
- Guest, B., Niemi, N., and Wernicke, B., 2007, Stateline fault system: A new component of the Miocene–Quaternary Eastern California shear zone: Geological Society of America Bulletin, v. 119, p. 1337–1347, https://doi .org/10.1130/0016-7606(2007)119[1337:SFSANC]2 .0.CO:2.
- Hammer, Ø., Harper, D.A.T., and Ryan, P.D., 2001, PAST: Paleontological Statistics software package for education and data analysis: Palaeontologia Electronica, v. 4, no. 1.
- Handley, J.C., Sheets, H.D., and Mitchell, C.E., 2009, Probability models for stasis and change in paleocommunity structure: Palaios, v. 24, p. 638–649, https://doi.org/10.2110/palo.2008.p08-109r.
- Heusser, L.E., Barron, J.A., Blake, G.H., and Nichols, J., 2022, Miocene terrestrial paleoclimates inferred from pollen in the Monterey Formation, Naples Coastal Bluffs section, California, in Aiello, I.W., Barron, J.A., and Ravelo, A.C., eds., Understanding the Monterey Formation and Similar Biosiliceous Units across Space and Time: Geological Society of America Special Paper 556, p. 215– 227, https://doi.org/10.1130/2022.2556(09).
- Hilgen, F.J., Lourens, L.J., and Dam, J.A.V., 2012, The Neogene Period, in Gradstein, F.M., Ogg, J.G., Schmitz, M.D., and Ogg, G.M., eds., The Geologic Time Scale: Amsterdam, Elsevier, p. 923–978, https://doi.org/10 .1016/B978-0-444-59425-9.00029-9.
- Holland, S.M., 2016, The non-uniformity of fossil preservation: Philosophical Transactions of the Royal Society B: Biological Sciences, v. 371.
- Holland, S.M., and Loughney, K.M., 2021, The Stratigraphic Paleobiology of Nonmarine Systems: Cambridge, UK, Cambridge University Press, Elements of Paleobiology Series, 82 p.
- Janis, C.M., 1993, Tertiary mammal evolution in the context of changing climates, vegetation, and tectonic events: Annual Review of Ecology, Evolution, and Systematics, v. 24, p. 467–500, https://doi.org/10.1146/annurev .es.24.110193.002343.
- Janis, C.M., Damuth, J., and Theodor, J.M., 2000, Miocene ungulates and terrestrial primary productivity: Where have all the browsers gone?: Proceedings of the National Academy of Sciences of the United States of America, v. 97, no. 14, p. 7899–7904, https://doi.org/10.1073/pnas.97.14.7899.
- Janis, C.M., Damuth, J., and Theodor, J.M., 2002, The origins and evolution of the North American grassland biome: The story from the hoofed mammals: Palaeogeography, Palaeoclimatology, Palaeoecology, v. 177, p. 183–198, https://doi.org/10.1016/S0031-0182(01)00359-5.
- Kisel, Y., McInnes, L., Toomey, N.H., and Orme, C.D., 2011, How diversification rates and diversity limits combine to create large-scale species-area relationships: Philosophical Transactions of the Royal Society B: Biological Sciences, v. 366, no. 1577, p. 2514–2525, https://doi .org/10.1098/rstb.2011.0022.
- Knott, J.R., Sarna-Wojcicki, A.M., Barron, J.A., Wan, E., Heizler, L., and Martinez, P., 2022, Tephrochronology of the Miocene Monterey and Modelo formations, California, understanding the Monterey Formation and similar biosiliceous units across space and time, in Aiello, I.W., Barron, J.A., and Ravelo, A.C., eds., Understanding the Monterey Formation and Similar Biosiliceous Units across Space and Time: Geological Society of America Special Paper 556, p. 187–214, https://doi.org /10.1130/2022.2556(08).
- Koch, P.L., Fogel, M.L., and Tuross, N., 1994, Tracing the diets of fossil animals using stable isotopes, in Lajtha, K., and Michener, R., eds., Stable Isotopes in Ecology and Environmental Science: Boston, Massachusetts, Blackwell Scientific.
- Kohn, M.J., and Fremd, T.J., 2008, Miocene tectonics and climate forcing of biodiversity, western United States:

- Geology, v. 36, p. 783–786, https://doi.org/10.1130/G24928A.1.
- Lechler, A.R., Niemi, N.A., Hren, M.T., and Lohmann, K.C., 2013, Paleoelevation estimates for the northern and central proto-Basin and Range from carbonate clumped isotope thermometry: Tectonics, v. 32, no. 3, p. 295–316, https://doi.org/10.1002/tect.20016.
- Leeder, M.R., 1993, Tectonic controls upon drainage basin development, river channel migration and alluvial architecture: Implications for hydrocarbon reservoir development and characterization, in North, C.P., and Prosser, D.J., eds., Characterization of Fluvial and Aeolian Reservoirs: Geological Society, London, Special Publication 73, p. 7–22.
- Loomis, D.P., and Burbank, D.W., 1988, The stratigraphic evolution of the El Paso basin, southern California: Implications for the Miocene development of the Garlock fault and uplift of the Sierra Nevada: Geological Society of America Bulletin, v. 100, p. 12–28, https://doi.org/10.1130/0016-7606(1988)100<0012:TSEO TE>2.3.CO;2.
- Loughney, K.M., and Badgley, C., 2017, Facies, environments, and fossil preservation in the Barstow Formation, Mojave Desert, California: Palaios, v. 32, p. 396–412, https://doi.org/10.2110/palo.2017.008.
- Loughney, K.M., and Badgley, C., 2020, The influence of depositional environment and basin history on the taphonomy of mammalian assemblages from the Barstow Formation (middle Miocene), California: Palaios, v. 35, no. 4, p. 175–190, https://doi.org/10.2110/palo .2019.067.
- Loughney, K.M., Badgley, C., Bahadori, A., Holt, W.E., and Rasbury, E.T., 2021, Tectonic influence on Cenozoic mammal richness and sedimentation history of the Basin and Range, western North America: Science Advances, v. 7, https://doi.org/10.1126/sciadv.abh4470.
- Lourens, E., Hilgen, F., Shackleton, N.J., Laskar, J., and Wilson, D., 2004, The Neogene Period, in Gradstein, F., Ogg, J., and Smith, A., eds., A Geologic Time Scale: Cambridge, UK, Cambridge University Press, p. 409–440.
- Marshall, C.R., 1990, Confidence intervals on stratigraphic ranges: Paleobiology, v. 16, no. 1, p. 1–10, https://doi.org/10.1017/S0094837300009672.
- Marshall, C.R., 2010, Using confidence intervals to quantify the uncertainty in the end-points of stratigraphic ranges, in Alroy, J., and Hunt, G., eds., Quantitative Methods in Paleobiology: The Paleontological Society Papers, v. 16, p. 291–316, https://doi.org/10.1017/S1089332600001911.
- McQuarrie, N., and Wernicke, B.P., 2005, An animated tectonic reconstruction of southwestern North America since 36 Ma: Geosphere, v. 1, p. 147–172, https://doi.org/10.1130/GES00016.1.
- Merriam, J.C., 1919, Tertiary mammalian faunas of the Mohave Desert: University of California Publications, Department of Geology Bulletin, v. 10, p. 111–127.
- Mitchell, A.H.G., and Reading, H.G., 1978, Sedimentation and tectonics, in Reading, H.G., ed., Sedimentary Environments and Facies: New York, Elsevier, p. 471–518.
- Pagnac, D., 2009, Revised large mammal biostratigraphy and biochronology of the Barstow Formation (Middle Miocene), California: PaleoBios, v. 29, no. 2, p. 48–59, https://doi.org/10.5070/P9292021802.
- Paola, C., Hellert, P.L., and Angevine, C.L., 1992, The large-scale dynamics of grain-size variation in alluvial basins, 1: Theory: Basin Research, v. 4, p. 73–90, https://doi.org/10.1111/j.1365-2117.1992.tb00145.x.
- Perkins, M.E., and Nash, B.P., 2002, Explosive silicic volcanisms of the Yellowstone hotspot: The ash fall tuff record: Geological Society of America Bulletin, v. 114, p. 367–381, https://doi.org/10.1130/0016-7606(2002)114<0367:ESVOTY>2.0.CO;2.
- Perkins, M.E., Brown, F.H., Nash, W.P., McIntosh, W., and Williams, S.K., 1998, Sequence, age, and source of silicic fallout tuffs in middle to late Miocene basins of the northern Basin and Range province: Geological Society of America Bulletin, v. 110, p. 344–360, https://doi .org/10.1130/0016-7606(1998)110<0344:SAASOS>2 .3.CO;2.
- Poage, M.A., and Chamberlain, C.P., 2002, Stable isotopic evidence for a pre-middle Miocene rain shadow in the

- western Basin and Range: Implications for the paleotopography of the Sierra Nevada: Tectonics, v. 21, no. 4, https://doi.org/10.1029/2001TC001303.
- Priego-Vargas, J., Bravo-Cuevas, V.M., and Jiménez-Hidalgo, E., 2016, The record of Cenozoic horses in Mexico: Current knowledge and palaeobiological implications: Palaeobiodiversity and Palaeoenvironments, v. 96, no. 2, p. 305–331, https://doi.org/10.1007/s12549-015-0223-y.
- Prothero, D.R., Domning, D., Fordyce, R.E., Foss, S., Janis, C., Lucas, S., Marriott, K.L., Metais, G., Naish, D., Padian, K., Rössner, G., Solounias, N., Spaulding, M., Stucky, R.M., Theodor, J., and Uhen, M., 2022, On the unnecessary and misleading taxon "Cetartiodactyla": Journal of Mammalian Evolution, v. 29, no. 1, p. 93–97, https://doi.org/10.1007/s10914-021-09572-7.
- Quade, J., Cerling, T.E., Barry, J.C., Morgan, M.E., Pilbeam, D.R., Chivas, A.R., Lee-Thopr, J.A., and van der Merwe, N.J., 1992, A 16-Ma record of paleodiet using carbon and oxygen isotopes in fossil teeth from Pakistan: Chemical Geology, v. 94, p. 183–192, https://doi.org/10 .1016/S0009-2541(10)80003-8.
- Renne, P.R., Mundil, R., Balco, G., Min, K., and Ludwig, K.R., 2010, Joint determination of <sup>40</sup>K decay constants and <sup>40</sup>Ar\*/<sup>40</sup>K for the Fish Canyon sanidine standard, and improved accuracy for <sup>40</sup>Ar/<sup>39</sup>Ar geochronology: Geochimica et Cosmochimica Acta, v. 74, p. 5349–5367, https://doi.org/10.1016/j.gca.2010.06.017.
- Rust, B.R., and Koster, E.H., 1984, Coarse alluvial deposits, in Walker, R.G., ed., Facies Models: Geological Association of Canada/Association géologique du Canada, p. 53–69.
- Schaen, A.J., et al., 2021, Interpreting and reporting <sup>40</sup>Ar/<sup>39</sup>Ar geochronologic data: Geological Society of America Bulletin, v. 133, p. 461–487, https://doi.org/10.1130/B35560.1.
- Smiley, T.M., 2016, Changes in small-mammal diversity and ecology in relation to landscape and climate change over the Neogene: Frontiers of Biogeography, v. 8, no. 4, https://doi.org/10.21425/F58432713.
- Smiley, T.M., Hyland, E.G., Cotton, J.M., and Reynolds, R.E., 2018, Evidence of early C4 grasses, habitat heterogeneity, and faunal response during the Miocene Climatic Optimum in the Mojave region: Palaeogeogra-

- phy, Palaeoclimatology, Palaeoecology, v. 490, p. 415–430, https://doi.org/10.1016/j.palaeo.2017.11.020.
- Smith, E.I., Sánchez, A., Keenan, D.L., and Monastero, F.C., 2002, Stratigraphy and geochemistry of volcanic rocks in the Lava Mountains, California: Implications for the Miocene development of the Garlock fault, Geologic evolution of the Mojave Desert and southwestern Basin and Range, in Glazner, A.F., Walker, J.D., and Bartley, J.M., eds., Geologic Evolution of the Mojave Desert and Southwestern Basin and Range: Geological Society of America Memoir 195, https://doi.org/10.1130 /0-8137-1195-9.151.
- Steinthorsdottir, M., et al., 2021, The Miocene: The future of the past: Paleoceanography and Paleoclimatology, v. 36, no. 4, https://doi.org/10.1029/2020PA004037.
- Strauss, D., and Sadler, P.M., 1989, Classical confidence intervals and Bayesian probability estimates for ends of local taxon ranges: Mathematical Geology, v. 21, p. 411–427, https://doi.org/10.1007/BF00897326.
- Tedford, R.H., 1965, Clarendonian faunal succession, Ricardo Formation, Kern County, California, in Abstracts for 1965: Abstracts of Papers Submitted for Six Meetings with Which the Society Was Associated: Geological Society of America Special Paper 87, p. 174, https://doi.org/10.1130/SPE87.
- Tedford, R.H., and Wang, X., 2009, Phylogenetic systematics of the North American fossil Caninae (Carnivora: Canidae): Bulletin of the American Museum of Natural History, v. 325, p. 1–218 p., https://doi.org/10.1206/574 1
- Tedford, R.H., Albright, L.B., Barnosky, A.D., Ferrusquia-Villafranca, I., Hunt, R.M., Storer, J.E., Swisher, C.C., Voorhes, M.R., Webb, S.D., and Whistler, D.P., 2004, Mammalian biochronology of the Arikareean through Hemphillian intervals (late Oligocene through early Pliocene epochs), in Woodburne, M.O., ed., Late Cretaceous and Cenozoic Mammals in North America: Biostratigraphy and Geochronology: New York, Columbia University Press, p. 169–231, https://doi.org/10.7312/wood13040-008.
- Tseng, Z.J., Takeuchi, G.T., and Wang, X., 2010, Discovery of the upper dentition of Barbourofelis whitfordi (Nimravidae, Carnivora) and an evaluation of the genus in California: Journal of Vertebrate Paleontology, v. 30, no. 1, p. 244–254, https://doi.org/10.1080/02724630903416001.

- Wang, X., and Barnes, L.G., 2008, Geology and Vertebrate Paleontology of Western and Southern North America: Contributions in Honor of David P. Whistler, Volume 41: Los Angeles, Natural History Museum of Los Angeles County, 388 p.
- Whistler, D.P., and Burbank, D.W., 1992, Miocene biostratigraphy and biochronology of the Dove Spring Formation, Mojave Desert, California, and characterization of the Clarendonian mammal age (late Miocene) in California: Geological Society of America Bulletin, v. 104, p. 644–658, https://doi.org/10.1130/0016-7606(1992)104<0644:MBAB OT>2.3.CO:2.
- Whistler, D.P., Tedford, R.H., Takeuchi, G.T., Wang, X., Tseng, Z.J., and Perkins, M.E., 2009, Revised Miocene biostratigraphy and biochronology of the Dove Spring Formation, Mojave Desert, California: Museum of Northern Arizona Bulletin, v. 65, p. 331–362.
- Whistler, D.P., Takeuchi, G.T., Groves, L.T., and Wang, X., 2013, Western Mojave Desert geology and vertebrate paleontology with special emphasis on the Dove Spring Formation: Society of Vertebrate Paleontology Field Trip Guidebook, 76 p.
- Wing, S.L., 1998, Tertiary vegetation of North America as a context for mammalian evolution, in Janis, C.M., Scott, K.M., and Jacobs, L.L., eds., Evolution of Tertiary Mammals of North America: Cambridge, UK, Cambridge University Press, p. 37–60.
- Woodburne, M.O., 1987, Cenozoic Mammals of North America: Berkeley, University of California Press, 336 p.
- Woodburne, M.O., ed., 2004, Late Cretaceous and Cenozoic Mammals of North America: Biostratigraphy and Geochronology: New York, Columbia University Press, 376 p., https://doi.org/10.7312/wood13040.
- Zachos, J., Pagani, M., Sloan, L., Thomas, E., and Billups, K., 2001, Trends, rhythms, and aberrations in global climate 65 Ma to Present: Science, v. 292, no. 5517, p. 686–693, https://doi.org/10.1126/science.1059412.

SCIENCE EDITOR: BRAD SINGER ASSOCIATE EDITOR: ROSS SECORD

Manuscript Received 14 April 2023 Revised Manuscript Received 8 September 2023 Manuscript Accepted 2 October 2023